



**HAL**  
open science

## Autonomous Industrial IoT for Civil Engineering Structural Health Monitoring

Gaël Loubet, Alassane Sidibe, Philippe Herail, Alexandru Takacs, Daniela Dragomirescu

► **To cite this version:**

Gaël Loubet, Alassane Sidibe, Philippe Herail, Alexandru Takacs, Daniela Dragomirescu. Autonomous Industrial IoT for Civil Engineering Structural Health Monitoring. IEEE Internet of Things Journal, 2024, 11 (5), pp.8921 - 8944. 10.1109/JIOT.2023.3321958 . hal-04247382

**HAL Id: hal-04247382**

**<https://laas.hal.science/hal-04247382>**

Submitted on 18 Oct 2023

**HAL** is a multi-disciplinary open access archive for the deposit and dissemination of scientific research documents, whether they are published or not. The documents may come from teaching and research institutions in France or abroad, or from public or private research centers.

L'archive ouverte pluridisciplinaire **HAL**, est destinée au dépôt et à la diffusion de documents scientifiques de niveau recherche, publiés ou non, émanant des établissements d'enseignement et de recherche français ou étrangers, des laboratoires publics ou privés.



Distributed under a Creative Commons Attribution - NoDerivatives 4.0 International License

# Autonomous Industrial IoT for Civil Engineering Structural Health Monitoring

Gaël LOUBET, *Member, IEEE*, Alassane SIDIBE, *Member, IEEE*, Philippe HERAIL, Alexandru TAKACS, *Member, IEEE*, and Daniela DRAGOMIRESCU, *Senior Member, IEEE*

**Abstract**— This paper presents a wireless Sensing Node part of a Wireless Sensor Network dedicated to the deployment of a Cyber-Physical System intended for the Structural Health Monitoring of reinforced concretes. This low-power Sensing Node requires less than 21 mJ for a full processing: measurement, data formatting and transmission of a 17 bytes LoRaWAN frame; *id est* 39  $\mu$ J per transmitted bit. It is designed to be buried in reinforced concrete and is battery-free and energy autonomous for long-term deployment by a radiative electromagnetic Wireless Power Transfer approach. The Sensing Node is cold-start compatible down to a power of -17 dBm available at the output of the antenna. It is able to wirelessly transmit data over at least tens of meters thanks to the LoRaWAN wireless communication technology. Moreover, it is wirelessly, remotely and omnidirectionally powered and controlled by a Communicating Node over meters, with the respect of regional regulatory constraints (Equivalent Isotropic Radiated Power of +33 dBm allowed in the 868 MHz Industrial, Scientific and Medical frequency band). By being a generic platform, this Sensing Node can employ various sensors to measure relevant parameters for the targeted application, *id est*: temperature, relative humidity, mechanical deformation through the strain, and electrical resistivity whose the variation allows to estimate the corrosion rate. By simultaneously using the same 868 MHz Industrial, Scientific and Medical frequency band for the wireless communication and the Wireless Power Transfer, the Sensing Node meets the Simultaneous Wireless Information and Power Transfer paradigm with a unique antenna and without interferences. Thus, the tested system allows the deployment of the subnetwork of two Communicating Nodes and several Sensing Nodes (currently four) to cover a surface/volume of several meters, currently up to 11 meters around each Communicating Node indoors. Finally, this system can be easily deployed for other applications requiring energy autonomous Wireless Sensor Networks, especially in harsh environments, such as reinforced concretes, space, underground mining, power plants, etc.

This work was supported in part by the French National Research Agency (ANR) under the McBIM project (Communicating Material at the disposal of the Building Information Modeling), grant number ANR-17-CE10-0014, and in part by the Région Occitanie under the OPTENLOC project.

(Corresponding authors: Gaël LOUBET, and Daniela DRAGOMIRESCU)

Gaël LOUBET is with LAAS-CNRS, Université de Toulouse, CNRS, INSA, 31400 Toulouse, FRANCE (e-mail: gael.loubet@laas.fr).

Alassane SIDIBE is with LAAS-CNRS, Université de Toulouse, CNRS, UWINLOC, 31400 Toulouse, FRANCE (e-mail: alassane.sidibe@laas.fr).

Philippe HERAIL is with LAAS-CNRS, Université de Toulouse, CNRS, 31400 Toulouse, FRANCE (e-mail: philippe.herail@laas.fr).

Alexandru TAKACS is with LAAS-CNRS, Université de Toulouse, CNRS, UPS, 31400 Toulouse, FRANCE (e-mail: alexandru.takacs@laas.fr).

Daniela DRAGOMIRESCU is with LAAS-CNRS, Université de Toulouse, CNRS, INSA, 31400 Toulouse, FRANCE (e-mail: daniela.dragomirescu@laas.fr).

**Index Terms**— Industrial Internet of Things (IIoT), Cyber-Physical System (CPS), Non-Destructive Testing (NDT), Structural Health Monitoring (SHM), Simultaneous Wireless Information and Power Transfer (SWIPT), Wireless Communications, Wireless Sensor Network (WSN), Wireless Power Transfer (WPT).

## I. INTRODUCTION

IN recent decades, the digitalization and miniaturization of electronics have led to a huge increase in the use of embedded electronic systems. The main objective is to have more functionalities on less volume and less power consumed. In this trend, wireless communications have played a key role by allowing moving remote and wireless communications between humans and/or machines. Thus, the machine-to-machine (M2M) wireless communications have made possible the development of Wireless Sensor Networks (WSN) [1]. The latter can be employed to monitor and/or control the physical world, as well as to connect the physical and digital worlds, in what is called Cyber-Physical Systems (CPS) [2]. Moreover, these Wireless Sensor Networks are the basic building block of the Internet of Things (IoT) paradigm which aims to make the communicating devices ubiquitous [3].

No matter the targeted application, the long-term deployment of Wireless Sensor Networks is currently severely limited by their energy autonomy. A large part of the deployed Wireless Sensor Networks is based on the use of batteries (primary or secondary) as of right now. These have a restricted lifetime and their manual replacement is time-consuming and expensive. To ensure the long-term energy autonomy of Wireless Sensor Networks, ambient energy harvesting and Wireless Power Transfer (WPT) solutions are investigated [4]. The ambient energy harvesting solutions are based on the scavenging of residual energy available in the environment. These energies can be light, mechanical/kinetic, thermal or electromagnetic. Nevertheless, these are highly dependent on the environment of deployment, fluctuating, unpredictable and uncontrollable. To overcome these limitations, a power source is used in Wireless Power Transfer solutions to make the scavenging of the specifically provided energy controllable, predictable, low fluctuating and low dependent on the environment of deployment. Currently, the Wireless Power Transfer solutions employ light, mechanical/kinetic and electromagnetic powers.

Regarding the electromagnetic Wireless Power Transfer, several technologies coexists: in near-field (capacitive, non-

resonant inductive and resonant inductive) and in far-field (radiative) [5]. Despite their high efficiencies and large variety of performances, near-field solutions have generally a short range of use (from millimeters to a few meters), which makes these unsuitable for Wireless Sensor Networks deployed in broad areas (*e.g.*, from rooms, to cities, through buildings) unlike far-field solutions. These last provide various performances usually dependent of the targeted application and of the regional regulations (both in terms of frequency bands and maximum Equivalent Isotropic Radiated Power (EIRP) allowed) [6] and achieve a range of use of at least several meters. By considering both the wireless communication and the radiative electromagnetic Wireless Power Transfer, some Wireless Sensor Networks meet the Simultaneous Wireless Information and Power Transfer (SWIPT) paradigm [7].

At the same time, Structural Health Monitoring (SHM) is becoming increasingly common in all application fields [8]. It consists in continuously overseeing the state of health of a thing, to prevent its irreversible failures, avoid its collapse, and allow to apply preventive treatments. To achieve it, Non-Destructive Testing (NDT) methods are privileged because these do not alter the element under test [9-11]. Also, the use of digital twins (such as a Building Information Modelling (BIM) in the civil engineering industry [12]) can be a relevant way to keep up-to-date a model of the element. The current and past information of these elements would be easily accessible for the different stakeholders (owners, users, etc.). Thus, Cyber-Physical Systems based on Wireless Sensor Networks are suitable for the implementation of autonomous Structural Health Monitoring applications in various fields.

Furthermore, the "communicating material" paradigm has been established [13]. This defines materials that are full Cyber-Physical Systems dedicated to Structural Health Monitoring applications in various fields. These are intrinsically able to: (1) measure (with Non-Destructive Testing methods), (2) process (locally and/or remotely), (3) store (locally and/or remotely) and (4) share (locally -with other communicating materials, Wireless Sensor Networks, or wireless communicating devices-, and/or remotely -especially with digital twins located in the digital world, through the Internet-) data characterizing their own internal health and/or their environment. This allows to have an updated follow-up of the materials and the structures to which these belong, during all their lifetime (from their manufacturing to their recycling, through their construction and exploitation). It also provides access to a history of the materials and the structures that is always accessible to authorized humans and/or machines.

In this context, the McBIM project (Material communicating with the Building Information Modelling), funded by the French National Research Agency (ANR), deals with the design and implementation of a communicating material for the civil engineering industry: a communicating reinforced concrete [14,15]. This is a full industrial Internet of Things system dedicated to Structural Health Monitoring of reinforced concretes and civil engineering structures. It is

based on an energy autonomous Wireless Sensor Network embedded in the material and able to update during all its life a Building Information Modelling available through the Internet. Due to a need for genericity (to be independent of the targeted environment and application) and due to the inaccessibility of the system once deployed in the material, a battery-free Wireless Sensor Network wirelessly powered by radiated electromagnetic waves has been chosen [16-18].

Thus, this paper focuses on the design, the implementation and the test of energy autonomous Sensing Nodes (SN), fully buried in reinforced concrete and part of a Wireless Sensor Network. These are battery-free, wirelessly and remotely powered and controlled, and capable of measuring and wirelessly transmitting relevant data for the Structural Health Monitoring of reinforced concretes. These communicate data over kilometers thanks to the LoRaWAN wireless communication technology and are wirelessly powered over several meters (at least up to 11 meters) in all the directions from a power source respecting the European regulations. By using simultaneously the 868 MHz Industrial, Scientific and Medical (ISM) frequency band for both the wireless communication and the Wireless Power Transfer, the proposed Sensing Nodes meet the Simultaneous Wireless Information and Power Transfer paradigm with a unique antenna.

Section II will address the designs of the Cyber-Physical System, and more specifically of the Sensing Nodes, by considering the current State of the Art in the various areas. Section III will deal with the characterization and test of the Sensing Nodes, and how the power consumption has been significantly reduced. Before concluding, Section IV will propose the analysis of the presented results, as well as will provide some axes of improvement and some future axes of research.

## II. ARCHITECTURES OF THE CYBER-PHYSICAL SYSTEM AND OF THE SENSING NODES

### A. Cyber-Physical System

The global architecture of the proposed Cyber-Physical System is presented in Fig. 1 [16-18]. Even though it was imagined for a communicating reinforced concrete, this Cyber-Physical System can be easily scalable to other communicating materials, as well as other Structural Health Monitoring applications, especially in harsh environments. Its physical part is a Wireless Sensor Network composed of two kinds of node, organized in a two-levels network. There are the Communicating Nodes (CN) and the Sensing Nodes (SN). Each element made of communicating material embeds at least one Communicating Node and several Sensing Nodes, this association forming a subnetwork. Their number is a function of the size of the element and the needs in terms of measurement (especially in terms of spatial precision).

The Communicating Nodes form an *ad-hoc* meshed network within a structure or a set of adjacent structures. These are intended to aggregate the data transmitted by the Sensing Nodes, then process, store and share it. The data can be

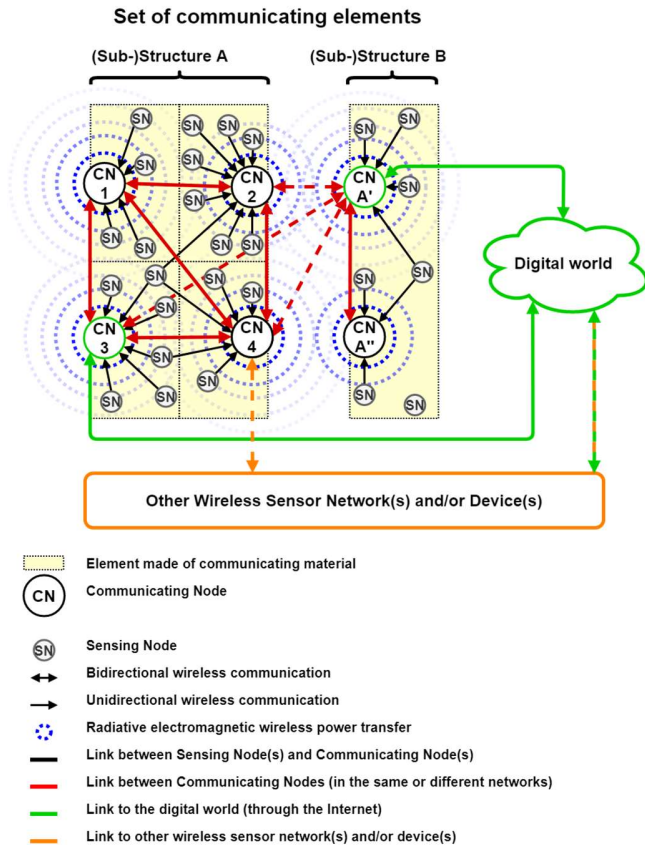


**Fig. 1.** Bloc diagram of the architecture of the Cyber-Physical System dedicated to the implementation of communicating materials.

processed, stored and shared locally in one or more Communicating Nodes of the network, and/or remotely in one or more other networks, in one or more other devices, or even in the digital world, and in particular in a digital twin, thanks to an access to the Internet. Thus, bi-directional medium to long range wireless communication technologies are required between the Communicating Nodes. Moreover, at least one Communicating Node per meshed network must be a reliable access point (or a gateway) to the digital world by providing a bi-directional connection to the Internet. Other bi-directional wireless communications technologies can be implemented to interface with other Wireless Sensor Networks and/or devices.

A star network of Sensing Nodes is available around each Communicating Node, thus, it becomes a central hub in a subnetwork. The Sensing Nodes are intended to measure relevant parameters of the monitored element and/or its environment. The collected data must then be transmitted to the associated Communicating Node(s) with directional medium range wireless communication technologies. In addition to the recovery of the data sent by the Sensing Nodes, the Communicating Nodes must wirelessly power the Sensing Nodes located in their neighborhood. By tuning their wireless power source (in terms of waveform, output power and/or periodicity of activation), the Communicating Nodes can set up the periodicity of functioning of the Sensing Nodes. A radiative electromagnetic Wireless Power Transfer system is

used to achieve this aim.

For the communicating reinforced concrete, a major part of the electromagnetic propagation medium (both for the wireless communication and the Wireless Power Transfer) is composed of reinforced concrete, which is highly constraining to the electromagnetic waves [19].

### B. Communicating Nodes

The Communicating Nodes must achieve several functions: (1) collect the data sent by the Sensing Nodes located in their neighborhood; (2) aggregate, process, store and share -locally and/or remotely- the data provided by the Sensing Nodes, by the other Communicating Nodes, by the other Wireless Sensor Networks and/or Devices, and/or by the digital twin(s); and (3) wirelessly power and control the Sensing Nodes located in their neighborhood, thanks to a Wireless Power Transfer system [16].

Thus, these are composed of two main subsystems: a radiative electromagnetic power source; and a control and data management and storage system, which also control the first subsystem. From another point of view, the Communicating Nodes present several interfaces, which require different performances (in terms of use, of directionality, of periodicity, of range, of data-rate, etc.) but which could be mutualized. These are: (1) for the collection of data from the Sensing Nodes; (2) for the Wireless Power Transfer; (3) for the communication with the other Communicating Nodes; (4) for the connection with the Internet; and (5) for each other types of wireless communication employed.

In the presented implementation, the Communicating Nodes are composed of a LoRaWAN gateway (based on a Raspberry Pi 3 model B+ from the Raspberry Pi Foundation (Caldecote, Cambridgeshire, United-Kingdom) and an iC880A LoRaWAN concentrator for IMST (Kamp-Lintfort, Germany), and using the Raspberry Pi OS Lite operating system from the Raspberry Pi Foundation (Caldecote, Cambridgeshire, United-Kingdom), the user datagram protocol packet-forwarder from Semtech (Camarillo, California, United States of America) and some Chirpstack tools (Orne Brocaar)) with Wi-Fi, Ethernet and cellular interfaces (a Bluetooth interface is available but not used) associated with a homemade power source (designed with components from Mini-Circuits (Brooklyn, New-York, United States of America)) providing a Continuous Wave (CW) signal with an Equivalent Isotropic Radiated Power of +33 dBm (or +3 dB, or 2 W) in the 868 MHz Industrial, Scientific and Medical frequency band [6]. More details on its implementation are available in [16].

### C. Sensing Nodes

The Sensing Nodes are the core elements of this Cyber-Physical System, because gathering the main constraints: inaccessibility (once deployed and embedded into the material), energy autonomy, fully wireless, long lifespan (that of the material itself (e.g., decades for reinforced concretes)), and so long-term usability, resilience and reliability [16-18].

## 1. Architecture

The architecture of the proposed Sensing Node is presented in Fig. 2. The Sensing Nodes are designed as simple as possible in order to minimize the risk of failure.

The Sensing Nodes must achieve one main function: sense some physical parameters to quantify the internal health state of the material and/or its environment, and wirelessly transmit the collected (and possibly pre-processed) data to the Communicating Node(s). Moreover, these must be energy autonomous for their entire lifetime, and thus, be battery-free and able to cold-start, and their periodicity of use must be controlled by the Communicating Nodes.

Therefore, these are composed of two distinct subsystems which interact: one dedicated to the power management and the other to the collection and transmission of data. The power management subsystem is composed of: a harvester (a rectenna, *i.e.* an antenna and a RF-to-DC rectifier, here connected through a radiofrequency circulator) used to harvest the radiative electromagnetic power generated and transmitted by the Communicating Node(s) and to convert it into DC electrical power; and a Power Management Unit (PMU) used to efficiently recover the power provided by the rectenna, to store it in energy storage buffer (here a supercapacitor), and to power the data management subsystem once enough energy is available. The data management subsystem is composed of a MicroController Unit (MCU) which drives a sensor and a wireless transceiver (here a LoRaWAN one) connected to the same antenna as for the power management subsystem (through the radiofrequency circulator). The aim is to measure physical parameter(s), pre-process the data and wirelessly send these to the Communicating Node(s) each time that the subsystem is powered.

Even though it could be attractive to send the raw data directly to further reduce the power consumption of the Sensing Nodes, a pre-processing step is specified to propose a generic system applicable to various use-cases. Generally, the power/energy consumption during processing time is much lower than during transmitting time. The overall power consumption of the Sensing Nodes can be reduced by limiting the amount of data to be sent and by minimizing the transmitting time. This may involve reducing the size of the data by reformatting or aggregating (e.g. averaging, pruning), in case of large format, or multiple data and/or data redundancy. Here, the pre-processing is just data reformatting

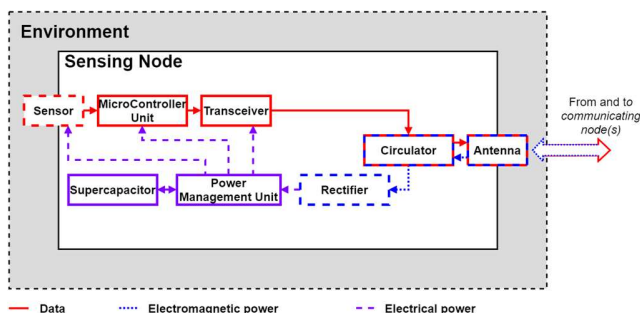


**Fig. 2.** Bloc diagram of the proposed generic architecture of the Sensing Node.

to reduce the size of the payload.

Finally, the proposed Sensing Node is well-suited for long-term deployment expressed in decades in harsh environments: (1) where maintenance is impractical because Sensing Nodes are inaccessible or difficult to access (e.g. buried in material, at very high heights, in satellites, in nuclear area, etc.); (2) which are isolated and without main power (e.g. desert, forests, mountains, etc.); (3) where batteries are unusable (e.g. explosive conditions, extreme temperatures, high humidity, radiations, dust, dirt, etc.) and ambient energy harvesting solutions unexploitable (e.g. caves, underground mining, etc.).

## 2. Design and Implementation

### a. Sensors

To certify standards, and mechanical or physical properties of concretes, these must be monitored on several parameters during their entire life. Even though the parameters to follow are different according to the step in the lifecycle (manufacture, curing, construction, exploitation, demolition, or recycling), some are more relevant and can be used during all the lifecycle: temperature, humidity, pH, corrosion, strain or stress, and cracks detection and location [9-11,20]. The main objective is to warranty a safe use of the material and of the structure, particularly by checking for their proper aging, and by detecting, locating and quantifying the damages, or even predicting these. This allows to perform maintenance or even predictive maintenance, when required and before the damages become irreversible.

In order to be implementable in Wireless Sensor Networks and to allow a continuous (with slowly evolving parameters), automatic and remote monitoring, the destructive (or semi-destructive) testing methods are rejected in favor of Non-Destructive Testing methods [9-11,20]. Moreover, to limit the needs in terms of energy and computing capacity, the direct and temporally punctual measurement methods are privileged and the methods requiring signal processing and/or energy-consuming equipment are discarded. Also, the proposed Sensing Nodes are based on a generic platform where different kinds of low-power sensors can be connected.

Currently, four different kinds of sensors have been successfully implemented and tested: temperature, temperature and relative humidity, strain, and dielectric resistivity; which are presented in Fig. 3.

The temperature, and temperature and relative humidity sensors deal with physical parameters. Considered together, these two physical parameters can be used in various applications during all the life of reinforced concretes, especially for the curing and the exploitation phases. Both academic and commercially available sensors have been used:

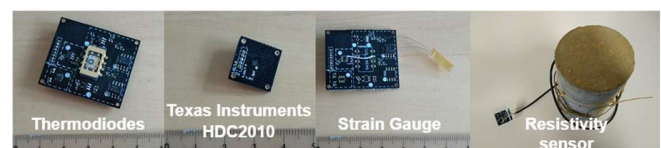


**Fig. 3.** Photographs of the daughter boards dedicated to the implementation of different sensors.

in particular thermodiodes from the University of Cambridge (Cambridge, United-Kingdom) as temperature sensors [21], and HDC2010 from Texas Instruments (Dallas, Texas, United States of America) as a temperature and relative humidity sensor [22]. These are supplied with a 3.3 V supply voltage, consume respectively 600  $\mu$ W and 200 nW on stand-by, and present measurement ranges between -40 °C and +125 °C with an accuracy of  $\pm 0.2$  °C (temperature) and 0 % to 100 % with an accuracy of  $\pm 2$  % (relative humidity, if applicable).

The strain sensor deals with a mechanical parameter: the strain. This mechanical parameter can be used in various applications during all the life of reinforced concretes to estimate the mechanical deformation. A commercially available simple and low-cost wire lead strain gauge has been used as a proof-of-concept [23]. This is supplied with a 3.3 V supply voltage and consumes 1.46 mW on stand-by.

The dielectric resistivity sensor deals with a chemical parameter: the corrosion. The corrosion rate can be estimated by the study of the evolution of the dielectric resistivity over time. This chemical parameter can be used in various applications during all the life of reinforced concretes. A fully buried academic Wenner probe from the Laboratory for Materials and Durability of Constructions (LMDC, Toulouse, France) has been used [24]. This is supplied with a 3.3 V supply voltage and consumes 580  $\mu$ W on stand-by.

Although the Structural Health Monitoring of reinforced concretes can be achieved during the major part of their lifecycle by correlating the data provided by all the implemented sensors, other kinds of sensors could be investigated [9-11,20]. Furthermore, some improvements could be achieved in order to maximize the accuracy and/or the range, while minimizing the power consumption.

#### b. Microcontroller Unit and Wireless Transceiver

To drive the sensor, and to process and transmit the data, a MicroController Unit driving a wireless transceiver must be implemented in the Sensing Nodes. Indeed, these must transmit at low power the few bytes of data collected over at least a few tens of meters from inside the material (here reinforced concrete) to the Communicating Node(s). Thus, for reasons of hardware security (fixed firmware and no access to alter or update it) and power consumption (no time dedicated to the listening of the communication medium), only the data uplink in a configuration which does not require connection or acknowledgement is used. Consequently, the Sensing Nodes are not able to receive data. There are several solutions that can be employed for these wireless transmissions.

Electromagnetic wireless communications technologies [1] have been selected in contrary of those based on the light [25] or the mechanical [26-28] waves, because: these provide no commercially available solutions; and cannot be efficiently used at medium to long ranges through all the media (*e.g.*, light in the reinforced concrete and mechanical waves in the air). Among the wide variety of technologies available, the focus has been on the Wireless Personal Area Networks (WPAN) [29] (*e.g.*, Bluetooth (IEEE 802.15.1 [30]), Bluetooth Low Energy (IEEE 802.15.1 [30]), ZigBee (IEEE 802.15.4

[31,32]), etc.) and the Low Power Wide Area Networks (LPWAN) [33] (*e.g.*, LoRaWAN [34], DASH7 (ISO 18000-7 [35]), etc.) for reasons of power consumption, data-rates, availability and range of use. For the future, and if commercially available, Ultra-Wide Band (UWB) (IEEE 802.15.3 [36,37]), and RuBee (IEEE 1902.1 [38]) (theoretically able to reliably communicate through reinforced concretes over ten meters), as well as mechanical communications (if the reinforced concrete is the propagation medium) are relevant investigation trends.

Preliminary qualitative tests for indoor wireless communications have been performed. This enabled the LoRaWAN technology to be chosen from among three representative wireless communication technologies tested without their operation being optimized in terms of power consumption: Bluetooth Low Energy, Ultra-Wide Band, and LoRaWAN. This choice was based on two criteria: (1) the range of use indoor, and especially the ability to pass through reinforced concrete walls and ceilings/floors, without loss of frame; (2) the power consumption in active mode. The Ultra-Wide Band solution based on the DW1000 transceiver from Qorvo (Greensboro, North Carolina, United States of America) has the shortest range (limited to a few meters) without the ability to pass through reinforced concrete, but also the highest power consumption in active mode: approximately 230 mW at 3.3 V. The Bluetooth Low Energy solution based on the nRF52832 module from Nordic Semiconductor (Trondheim, Norway) has a range of tens of meters with the ability to pass through some reinforced concrete elements, and for the lowest power consumption in active mode: approximately 25 mW at 3.3 V for a +3 dBm transmission. The LoRaWAN solution based on the SX1272 transceiver from Semtech (Camarillo, California, United States of America) has the longest range, easily exceeding a few hundreds of meters. It covers the entire LAAS-CNRS laboratory which is distributed over 4 levels with distances of a few hundreds of meters, and even well beyond, with the ability to pass through a lot of reinforced concrete elements without loss of frame, and for a power consumption in active mode: approximately 100 mW at 3.3 V for a +14 dBm transmission. That is considered low but remains relatively high compared with the Bluetooth Low Energy solution. At this stage, it appeared that a single LoRaWAN gateway was sufficient to cover more space than required, thanks to the Chirp Spread Spectrum (CSS) technique which appears not too sensitive to the reinforced concrete.

In terms of power consumption, LoRaWAN can be considered as one of the "worst" cases among LPWAN and WPAN technologies. Therefore, the success of its implementation (with its power supply by Wireless Power Transfer) will provide one of the "worst" characteristics, only improvable, and will certify the possibility to use technologies requiring less energy. For this reason, some experimentations with Bluetooth Low Energy have already been successfully carried out with similar Sensing Nodes [39].

Because compact, inexpensive and complete, an all-in-one CMWX1ZZABZ-091 LoRaWAN module from Murata

(Nagaokakyōshi, Kyoto, Japan) [40] (based on an SX1276 LoRa transceiver from Semtech (Camarillo, California, United States of America) [41] and a STM32L072CZ microcontroller from STMicroelectronics (Amsterdam, Netherlands) [42]) requiring a 3.3 V voltage supply has been used. Nevertheless, solutions based on independent MicroController Unit and LoRa transceiver could allow a wider design flexibility at the price of a more complex system. To provide a generic platform, all the interfaces are made available for the connection of all kinds of sensors. The firmware developed in C and employing the LoRaWAN stack provided by Semtech (Camarillo, California, United States of America) is reduced to a one-shot measurement and a LoRaWAN transmission. This measurement process starts with the initialization of the MicroController Unit, interfaces and desired peripherals; followed by the control of the sensor to obtain the measurement. Pre-processing of the data to format it as a 2-byte integer to get a generic and reduced data format regardless the kind of measurement, in particular to facilitate interfacing with partners is then performed. Before going into a deep-sleep mode, the formatted data is transmitted in a LoRaWAN frame. The all measurement and transmission process is depicted in Fig. 4. The LoRaWAN frames are 17 bytes long, whose 13 bytes dedicated to the LoRaWAN protocol and 4 bytes dedicated to the data payload. The payload can be reduced by optimizing the data formatting. A unique antenna is used both for the wireless communication and Wireless Power Transfer *via* a RF circulator, and will be presented later.

### c. Strategy of Use

Because the targeted periodicity of measurement is long (*e.g.*, once an hour, once a day, once a week, or once a month for the Structural Health Monitoring of reinforced concretes depending on the phase in the lifecycle) and considering that the available electromagnetic power is largely inferior to the DC electrical power required by the data management subsystem [43,44], a "store then use" strategy is applied. In this strategy, the scavenged power is stored, and once enough energy is available, this is used to power the data management subsystem, as presented in Fig. 4. That way, the periodicity is not controlled by the software (*e.g.*, with events or timer

interruptions) but by the hardware *via* the power management subsystem. Thus, to design the power management part of the Sensing Nodes, it is necessary to know the energy these require to work properly. In any case, the minimization of the energy needed to operate the system is targeted, and can be achieved in both software and hardware.

### d. Implementation of the Wireless Power Transfer

To be controllable, predictable, low fluctuating and low dependent on the environment of deployment, a Wireless Power Transfer solution is favored over ambient energy harvesting solutions, as presented in Fig. 5. For the same reasons as for wireless communications, the electromagnetic Wireless Power Transfer is favored over light (laser or infrared) and mechanical/kinetic (sonic and ultrasonic) Wireless Power Transfer solutions. Moreover, to achieve sufficiently wide ranges of use, near-field (capacitive, non-resonant inductive and resonant inductive) solutions are discarded in favor of far-field (radiative) solutions. Today, the radiative electromagnetic Wireless Power Transfer systems are oriented towards ubiquitous applications with very low power densities. This is partly because, on the one hand, there is a desire to reduce the global energy consumption, and on the other, it is to ensure the safety of living beings.

The range of use of the radiative electromagnetic Wireless Power Transfer is highly constrained by the choice of the frequency band, which is subject to regional regulations [6], and which is here chosen among the Industrial, Scientific and Medical radiofrequency bands. First, the free-space path losses (1) are function of the frequency: the higher the frequency, the larger the free-space losses, and the shorter the range of use. Second, the range of use (2) is a function of the transmitted power, whose maximum Equivalent Isotropic Radiated Power depends on regional regulations.

$$\text{free\_space\_path\_losses} = 20 \cdot \log\left(\frac{4\pi \cdot d \cdot f}{c}\right) \text{ (dB)} \quad (1)$$

$$\text{range} = \sqrt{\frac{\lambda^2}{4\pi} \cdot \frac{P_{EIRP}}{3600 \cdot \pi \cdot P_{IN}}} \text{ (m)} \quad (2)$$

with  $d$  the distance,  $f$  the frequency,  $c$  the celerity of light,  $\lambda$  the wavelength,  $P_{EIRP}$  the maximal Equivalent Isotropic Radiated Power (fixed by the regional regulations) and  $P_{IN}$  the minimum required input power.

According to Table I. which compares the use of different Industrial, Scientific and Medical frequency bands for the radiative electromagnetic Wireless Power Transfer, the most attractive frequency band, with the highest range of use for a defined input power (over meters), is the 868 MHz frequency band.

The power harvester for the electromagnetic waves is a rectenna, that says an antenna connected to a RF-to-DC rectifier. Its role is to efficiently harvest the radiative electromagnetic power generated by the Communicating Nodes (with a power density as low as possible); in order to provide a sufficient DC electrical power to allow the Power Management Unit and the energy buffer to efficiently and sufficiently store the energy; to finally use it to power the data

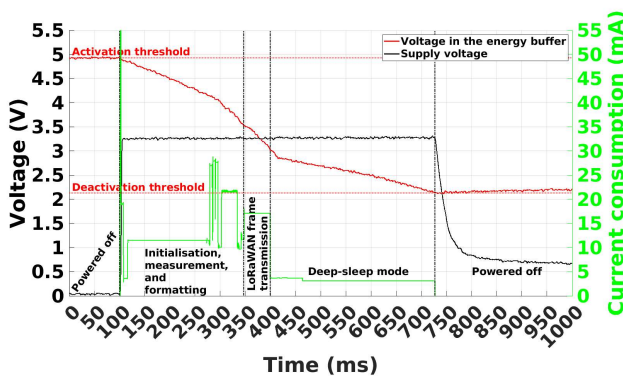


Fig. 4. Example of the power consumption of the sensing nodes according to the phase of operation.

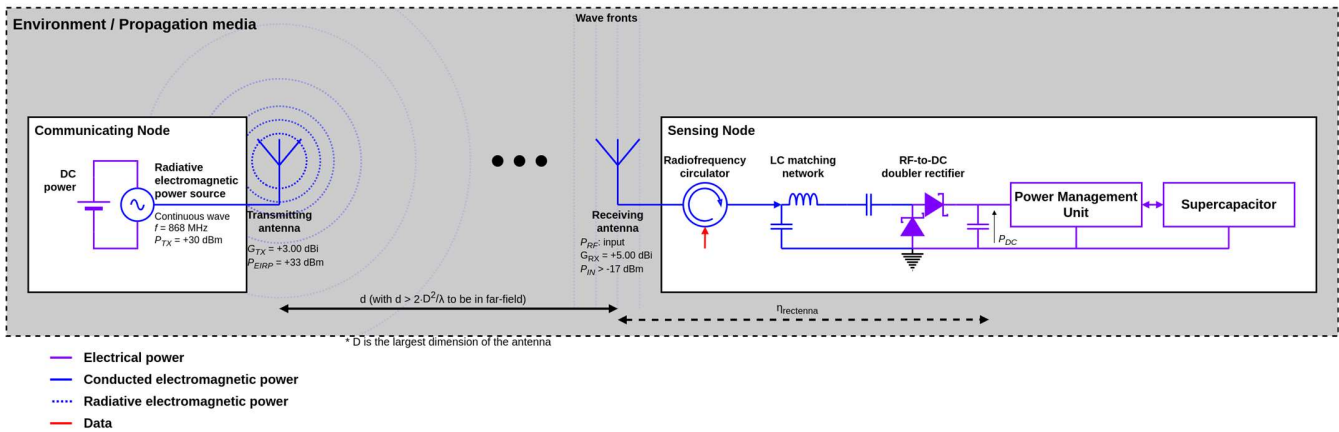


Fig. 5. Bloc diagram of the implementation of the Wireless Power Transfer solution.

management subsystem. This must be well designed to meet the properties of the transmitted power (e.g., power density level, central frequency, frequency band, polarization, etc.).

It must be noted that the overall size of the Sensing Nodes is correlated to the size of their antenna(s), which is closely

related to their wavelength/frequency: the higher the frequency, the smaller the antenna; and its bandwidth: the wider the bandwidth, the larger the antenna. Thus, the choice of the frequency band must also be a trade-off between the size of the Sensing Nodes *via* the size of the antenna(s) and the range of use. At 868 MHz, the size of the antenna stays usually small enough.

In order to reduce the overall size of the Sensing Nodes and because the same frequency band is used for both the wireless data communication and the Wireless Power Transfer, it has been chosen to employ a unique antenna for the two functions. As there is only data uplink and power downlink, it has been possible to use a radiofrequency circulator C11-1FFF/OPT.N from Aerotek (Hanover, Maryland, United States of America) [45], with low insertion losses and high isolation. This way, the power harvested by the antenna is transmitted to the rectifier through the radiofrequency circulator, and the data frame provided by the transceiver is transmitted to the antenna through the radiofrequency circulator simultaneously. In addition, there is no interconnection between the rectifier and the transceiver, and no interference between the data transfer and the power transfer.

The Communicating Nodes generate a Narrow-Band (NB) Continuous Wave at a frequency close to 868 MHz *via* their radiative electromagnetic power source. The Sensing Nodes and the Communicating Nodes use LoRa signal based on Chirp Spread Spectrum technique on one of the five defined subchannels in the 868 MHz Industrial, Scientific and Medical frequency band. On the Sensing Nodes side, the received input signal for the Wireless Power Transfer has a lower power level than the output one used for the data transmission. Thus, the output signal is not altered whatever the waveform of the input signal. Moreover, this behavior is further enhanced by the high isolation of the radiofrequency circulator between the output and input channels. So, there is no interference for the Sensing Nodes. On the Communicating Nodes side, the output signal for the Wireless Power Transfer is considered as noise by the LoRaWAN input frame receiver. There is also no interference thanks to the noise resistance of Chirp Spread Spectrum technique.

TABLE I

COMPARISON OF INDUSTRIAL, SCIENTIFIC AND MEDICAL FREQUENCY BANDS FOR THE DESIGN OF THE RADIATIVE ELECTROMAGNETIC WIRELESS POWER TRANSFER SYSTEM

Central frequency (MHz)	13.56	433	868	2,450	5,800
Wavelength in the air (cm)	2.210	69.2	34.4	12.2	5.2
Bandwidth (MHz)	0.014	1.74	5	100	150
Maximum EIRP [6] (dBm / mW)	N/A	+10 / 10	+33 / 2,000	+20 / 100	+23 / 200 or +30 / 1,000
Free-space losses at 1 m (dB)	N/A	25.17	31.21	40.23	47.71
Theoretical range for obtaining $P_{IN} = +0$ dBm (or 1 mW) at the output of a 0 dBi antenna for a power source generating a signal with maximum EIRP (cm)	N/A	17	123	9	6 or 13
Theoretical range for obtaining $P_{IN} = -14$ dBm (or 39.8 $\mu$ W) at the output of a 0 dBi antenna for a power source generating a signal with maximum EIRP (cm)	N/A	87	615	48	29 or 65
Theoretical range for obtaining $P_{IN} = -17$ dBm (or 20.0 $\mu$ W) at the output of a 0 dBi antenna for a power source generating a signal with maximum EIRP (cm)	N/A	123	869	68	41 or 92

Thus, a new solution and implementation of the Simultaneous Wireless Information and Power Transfer paradigm is provided, without temporal, frequential, or spatial multiplexing, neither power splitting, but with a discrimination/separation through the circulator of the sense of signal flows (data from the transceiver to the antenna and power from the antenna to the rectifier).

It must be noted that this solution does not increase the power consumption, for either the Sensing Nodes, or the Communicating Nodes, even in case of interferences. Indeed, the Sensing Nodes implement no data downlink, thus, cannot receive acknowledgment frames. In that way, no retransmission strategy is deployed, so, no increase in the power consumption can occur in case of interferences. The case of the loss of data (which eventually could be problematic) could be neglected thanks to spatial redundancy if enough Sensing Nodes are deployed. Finally, as long as the Communicating Nodes consider the Wireless Power Transfer signal as noise, there is no alteration of their nominal functioning, so, no increase in their power consumption.

The antenna must meet the best trade-off between its volume and its performances (radiation pattern, gain, polarization, etc.). The objective is to get Sensing Nodes as compact as possible, with the largest possible range of use for its wireless power supply, and whose functioning is as independent as possible from their location and orientation. In consequence, the ideal antenna must be compact, have a high gain and an isotropic/omnidirectional radiation pattern.

Thus, a printed folded quart-wavelength dipole antenna with capacitive arms has been chosen, as presented in Fig. 6 [46]. This has been designed on a FR4 substrates (thickness: 0.8 mm and 1.6 mm; relative permittivity: 4.4; and loss tangent: 0.02) and measures 5.6 cm x 3.2 cm x 1.0 cm. A folded quarter-wavelength dipole antenna with a short-circuited loop, to make a T-match structure, is used as a base, which allows an input impedance matching to 50  $\Omega$ , and a narrow-band and almost isotropic behavior. Metallic arms, orthogonal to the plane of the folded quarter-wavelength dipole antenna, are connected to each monopole which induces a capacitive coupling allowing to reduce the size of the antenna at the targeted frequency. This antenna is almost omnidirectional, has a linear polarization, is usable (*i.e.* impedance matched) between 848 MHz and 886 MHz, has a measured gain of +1.54 dBi at 868 MHz and has a measured -3 dB beamwidth of 110  $^\circ$  in the E-plane, as represented in Fig. 7. By adding an

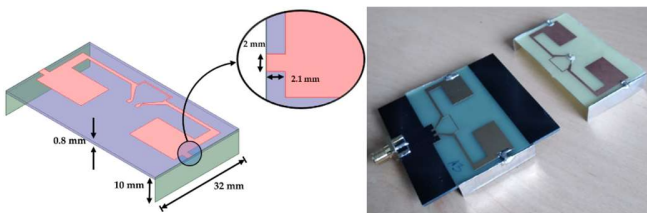


**Fig. 6.** Diagram and photograph of the designed and implemented printed folded quart-wavelength dipole antenna with capacitive arms at 868 MHz, on a 1.6 mm (black) and 0.8 mm (yellow) FR4 substrate.

8 cm x 6 cm metallic reflector plane at 5 cm from it, the measured gain is increased up to +5.00 dBi at the cost of the increase of the directionality and the rise of the volume. The measured -3 dB beamwidth is then 70  $^\circ$  in the E-plane. In addition, the first designs of this antenna on a flexible substrate (Kapton) have been completed, and have provided encouraging preliminary results.

Concerning the targeted application, the antenna must properly work in a particular environment: the reinforced concretes. It must be noted that the antenna has been successfully tested into a reinforced concrete beam, both for Wireless Power Transfer and wireless communication. Nevertheless, this was not in direct contact with the reinforced concrete but located in an air cavity. It is very probable that an impedance mismatch occurs when the antenna will be directly buried into the reinforced concrete, and a redesign must be provided by considering the reinforced concrete as the main propagation medium (thus, by considering its dielectric properties which may change during time). There are in the literature some works dealing with the study, the design, the manufacturing and the test of antenna buried into concretes [47-52].

The rectifier must meet the best trade-off between its efficiency, its characteristics (frequency/bandwidth, input impedance, typical range of available radiofrequency input powers, etc.) and its complexity (topology, size, non-linear rectifying component, etc.). The objective is to get a rectifier as efficient as possible especially for the lowest power densities, and provide a sufficient voltage to the Power Management Unit for optimum operation, both in the cold-start and in the normal charging modes. Also, the rectifier must be impedance matched with the associated antenna in the targeted frequency band and must be followed by a low pass filter in order to provide a DC voltage with a minimized ripple at the input of the Power Management Unit.

Therefore, a full-wave rectifier has been chosen, as presented in Fig. 8 [53]. This has been designed on a FR4 substrate (thickness: 0.8 mm and 1.6 mm; relative permittivity: 4.4; and loss tangent: 0.02) and optimized to be the most efficient for an input power of -15 dBm (or 31.6  $\mu$ W) in the Industrial, Scientific and Medical 868 MHz frequency band and for a 10 k $\Omega$  resistive load. This is based on a

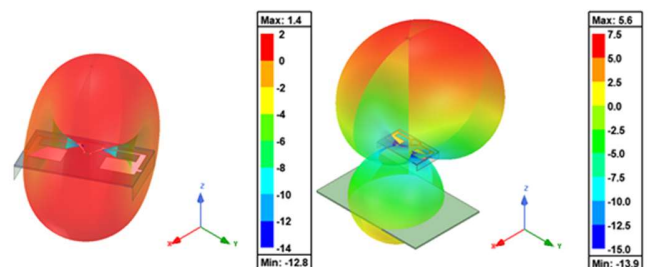


**Fig. 7.** Simulated (HFSS) radiation patterns of the printed folded quart-wavelength dipole antenna with capacitive arms at 868 MHz, with and without the use of a 6 cm x 8 cm metallic reflector plane located at 5 cm below the antenna/rectenna.

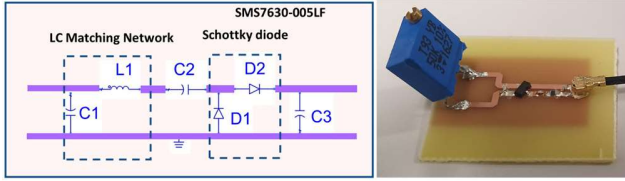


**Fig. 8.** Schematics and photograph of the designed and implemented full-wave rectifier on 0.8 mm thick FR4 substrate connected to a 10 k $\Omega$  load.

microstrip coupled transmission line allowing differential feeding, and on the use of two SMS7630 surface-mount Schottky diodes (on the SMS7630-005LF implementation) from Skyworks (Irvine, California, United States of America) [54], which are mounted in doubler configuration. A shunt surface mount capacitor is used at its output as a low-pass filter, whilst an 'L'-topology impedance matching network is used at its input. This last circuit is used in order to ensure the maximal power transfer from the antenna to the diodes, and is composed of a surface-mount inductor and a surface mount capacitor, both lumped, in order to get a 50  $\Omega$  impedance at the input of the full rectifier. The rectifier has a reflection coefficient ( $S_{11}$ ) of -19 dB at the input port, a nearly 330 mV output voltage, an almost 35 % efficiency (defined as the ratio between the output power on the input power), that says an output power of nearly 11  $\mu$ W for a -15 dBm (or 31.6  $\mu$ W) input, and has a 60 MHz bandwidth.

A rectenna composed of the printed folded quart-wavelength dipole antenna with capacitive arms (presented in Fig. 6) and of the full-wave rectifier designed for FR4 substrate (presented in Fig. 8) was designed and tested. Its efficiency ( $\eta_{rectenna}$ ) (3) for a 10 k $\Omega$  resistive load at 868 MHz, represented in Fig. 9, is computed thanks to the measured output DC power of the rectifier ( $P_{DC}$ ) and the estimated input radiative electromagnetic (or radiofrequency) power of the antenna ( $P_{RF}$ ) (4). This can also be expressed as the product of the incident electromagnetic power density ( $S$ ) (5) by the effective area of the antenna ( $A_{eff}$ ) (7). The incident

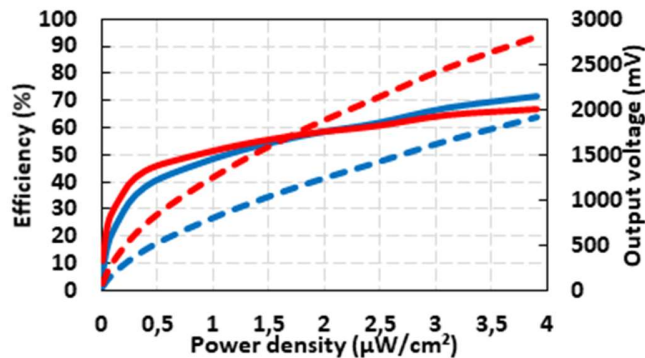


**Fig. 9.** Computed efficiency (full lines) and measured output DC voltage (dashed lines) against power densities for the printed folded quart-wavelength dipole rectenna with capacitive arms without (blue) and with (red) the use of a 6 cm x 8 cm reflector plane located at 5 cm below the antenna/rectenna, at 868 MHz and for a 10 k $\Omega$  resistive load.

electromagnetic power density ( $S$ ) (5) can be estimated thanks to the effective electric field ( $E$ ) (6) and the power generated by the radiative electromagnetic source ( $P_{TX}$ ), the gain of the antenna used by the radiative electromagnetic source ( $G_{TX}$ ), and the distance between the radiative electromagnetic source and the rectenna ( $d$ ). The effective area of the antenna ( $A_{eff}$ ) (7) can be estimated thanks to the gain of the antenna used by the rectenna ( $G_{RX}$ ) and the wavelength ( $\lambda$ ).

$$\eta_{rectenna} = \frac{P_{DC}}{P_{RF}} = \frac{P_{DC}}{S \cdot A_{eff}} = \frac{16 \cdot \pi^2 \cdot d^2}{P_{TX} \cdot G_{TX} \cdot G_{RX} \cdot \lambda^2} \cdot P_{DC} \quad (3)$$

$$P_{RF} = S \cdot A_{eff} = \frac{P_{TX} \cdot G_{TX} \cdot G_{RX} \cdot \lambda^2}{4 \cdot \pi \cdot d^2 \cdot 4 \cdot \pi} = \frac{P_{TX} \cdot G_{TX} \cdot G_{RX} \cdot \lambda^2}{16 \cdot \pi^2 \cdot d^2} \quad (W) \quad (4)$$

$$S = \frac{E^2}{120 \cdot \pi} = \frac{30 \cdot P_{TX} \cdot G_{TX}}{120 \cdot \pi \cdot d^2} = \frac{P_{TX} \cdot G_{TX}}{4 \cdot \pi \cdot d^2} \quad (W \cdot m^{-2}) \quad (5)$$

$$E = \frac{\sqrt{30 \cdot P_{TX} \cdot G_{TX}}}{d} \quad (V \cdot m^{-1}) \quad (6)$$

$$A_{eff} = G_{RX} \cdot \frac{\lambda^2}{4 \cdot \pi} \quad (m^2) \quad (7)$$

Several improvements can be achieved in order to increase the efficiency of the rectenna, concerning both the antenna and the rectifier, but also the connection between these.

#### e. Power Management Unit

To implement the "store then use" strategy, a Power Management Unit must be employed. This must efficiently scavenge the DC electrical power provided by the rectifier, efficiently store it in the energy buffer, and efficiently use the stored energy, once enough is available, to power the data management subsystem. It must properly work with the lowest possible input power and the lowest possible start-up voltage, but also present the lowest possible quiescent currents and sufficient output voltage and current.

A BQ25504 Power Management Unit from Texas Instruments (Dallas, Texas, United States of America) has been chosen [55]. This can be controlled through threshold voltages from the energy buffer, provide a hardware Maximum Power Point Tracking (MPPT) system to optimize the power transfer from the rectifier to the energy buffer, and is able to cold-start, therefore, to operate even with an empty energy buffer. In order to smooth out the current draw and to provide a 3.3 V constant voltage to the load when enough energy is available, as presented in Fig. 4, a TPS63031 DC-to-DC buck-boost converter from Texas Instruments (Dallas, Texas, United States of America) is used [56].

As presented in Fig. 10, if the energy buffer is empty, the Power Management Unit will use its cold-start ability to start storing the available input power in this last. When a sufficient voltage is reached, the hardware Maximal Power Point Tracking system is powered-up and will allow to optimize the power transfer from the input to the energy buffer. In fact, this circuit will sample the open-circuit input voltage every 16 seconds to impose on the input a ratio of it. This ratio is configurable with a resistor divider, and is currently set to 40 % of the open-circuit input voltage. Then, when the voltage in the energy buffer will reach the activation threshold, the power good indicator will be raised and will activate the

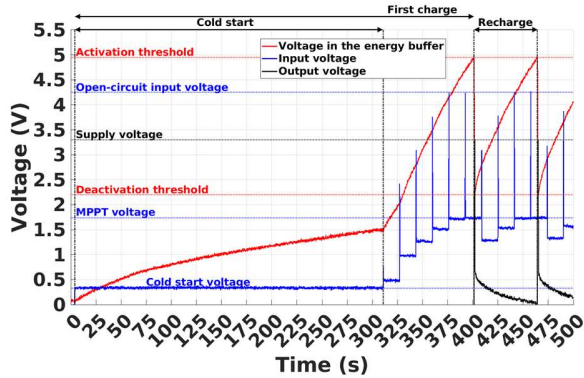


**Fig. 10.** Voltages, during a cold-start, a complete first charge and then a recharge, at the input of the Texas Instruments BQ25504 Power Management Unit (blue), in the energy buffer (red), and at the output of the Texas Instruments TPS63031 DC-to-DC buck-boost converter (black), for an input power of +0 dBm at 868 MHz.

power supply of the data management subsystem. The energy buffer will start its discharge. When the voltage in the energy buffer will reach the deactivation threshold, the power good indicator will be turned down and will deactivate the power supply of the data management subsystem. Thus, the activation and deactivation thresholds, configurable with resistor dividers, allow to control the charge and discharge levels of the energy buffer. And this process will be periodically done as long as sufficient power is available at the input. It must be noted that undervoltage (to prevent the deep discharge), overvoltage (to prevent the over charge) and overheating protection mechanisms are available and configurable with resistors.

To work properly, this Power Management Unit requires a typically 15  $\mu\text{W}$  input power during the cold-start and at least 10  $\mu\text{W}$  during the normal charging, and this DC-to-DC buck/boost converter has maximum losses of 4.725  $\mu\text{W}$  (disable and with an input power of 5.25 V) and 1.62  $\mu\text{W}$  at the end of the cold-start (with a voltage of 1.8 V). Thus, at least around 14.725  $\mu\text{W}$  are needed by these components to work properly during the normal charging, and 16.62  $\mu\text{W}$  during the cold-start. Some other Power Management Units requires less energy. This is the case for the BQ25505 [57] and BQ25570 [58] from Texas Instruments (Dallas, Texas, United States of America), which present the same behavior and similar performances, and which require a typically 15  $\mu\text{W}$  input power during the cold-start and at least 5  $\mu\text{W}$  during the normal charging. As well, the AEM30940 from e-peas (Mont-Saint-Guibert, Belgium) requires a typically 3  $\mu\text{W}$  input power during the cold-start and at least -19 dBm (or 12.5  $\mu\text{W}$ ) during the normal charging [58].

By properly designing the combination between the capacitance ( $C$ ) of the energy buffer and the activation ( $V_{act}$ ) and deactivation ( $V_{deac}$ ) thresholds voltage of the Power Management Unit, it is possible to ensure that enough energy ( $E$ ) is stored to correctly power the data management subsystem (8).

$$E = \frac{C}{2} \cdot (V_{act}^2 - V_{deact}^2) \quad (8)$$

#### f. Energy Buffer

Conjointly designed with the Power Management Unit, the energy buffer must be able to store enough energy to power supply the data management subsystem for an entire process, as presented in Fig. 4. Also, the Sensing Nodes must work for several decades and require some milli-joules to a few tens of milli-joules of energy to properly work. The required amount of energy is a function of the components (sensor, MicroController Unit, transceiver) and of their configuration (for the wireless communication: frequency band, output power, data-rate, etc.). Thus, to provide a battery-free solution, the choice fell on the supercapacitors (or eventually capacitors or bank of capacitors). Indeed, the batteries have a limited lifetime, must eventually be recharged, but also have too large capacitances, while supercapacitors (and capacitors or bank of capacitors) have a wide range of low to medium capacitances and theoretical very long lifetime (expressed in millions of cycles). In fact, the choice is made according to the targeted capacitance (related to the maximum activation and minimum deactivation threshold voltages of the Power Management Unit) and in order to minimize the self-discharge currents and losses. Regarding the technology, the supercapacitors that store the energy in an electrostatic way (e.g., electric double layer capacitors (EDLC)) have been favored, if available, over those that store the energy in an electro-chemical way (e.g., polarized aluminum electrolytic supercapacitors). This allows having a better ratio between energy and power densities, a longer lifetime, a lower self-discharge current and a lower sensitivity to the environment.

For the implementation of Sensing Nodes, two different supercapacitors have been employed related to the energy required and by adding a margin to compensate the variability between components and the alterations over time: a 22mF electric double layer capacitor from AVX Corporation BestCap (Greenville, South-Carolina, United States of America) [60] for storing up to 250 mJ, and a 2.2 mF polarized aluminum electrolytic supercapacitor from Panasonic (Kadoma, Osaka, Japan) [61] for storing up to 21 mJ. These have been chosen according to their capacitance and because providing the lowest self-discharge currents among the available solutions at the date of manufacturing. So, in the worst cases, the 22 mF supercapacitor requires 26  $\mu\text{W}$  to compensate its highest losses for the maximum activation threshold voltage and 9  $\mu\text{W}$  at the end of the cold-start, whilst respectively 606  $\mu\text{W}$  and 71  $\mu\text{W}$  for the 2.2 mF supercapacitor. Supercapacitors with higher capacitances could be used, but regarding the energy stored and unavailable (all the one under the deactivation threshold voltage), this is not relevant and even less energy efficient. Moreover, to be more energy efficient, the deactivation and activation threshold voltages must be minimized in order to limit the energy uselessly stored and to limit the maximum leakage current which is a function of the voltage.

#### g. Theoretical Estimation of the Range of Use

Currently, this is the Wireless Power Transfer which is limiting in terms of range of use and not the wireless communications. This limitation is imposed by the minimum input power required by the power management subsystem and its global efficiency. By considering the minimum power required by the power management subsystem to properly work (function of the rectenna efficiency, of the power required by the Power Management Unit, and of the power lost by the energy buffer), it is possible to estimate the maximum range of use in the worst case and for direct line of sight condition. This estimation is based on (3).

Thus, in the worst cases and with the 2.2 mF supercapacitor, a minimum input power of 87.62  $\mu\text{W}$  is required to be almost certain to obtain a proper work of the power management subsystem during the cold-start, and at least 620.725  $\mu\text{W}$  during the normal charging. With the 22 mF supercapacitor, these powers are respectively 25.62  $\mu\text{W}$  and 40.725  $\mu\text{W}$ . By using a model of the rectenna efficiency against power densities, based on the measured results presented in Fig. 9, and approximated by a logarithmic function for the lowest power densities (best correlation), it has been possible to estimate the minimum power density required in the worst use case for the normal charging and the cold-start, with the +1.54 dBi gain of the printed folded quart-wavelength dipole rectenna with capacitive arms, and for a +33 dBm (or +3 dB, or 2W) radiative electromagnetic power source at 868 MHz. From this value, the estimation of the maximum range of use of the Wireless Power Transfer system in this fixed configuration has been computed.

Thus, for the 2.2 mF supercapacitor, a power density of 1.205  $\mu\text{W}\cdot\text{cm}^{-2}$  (i.e. -7.87 dBm or 163.3  $\mu\text{W}$  harvested) for the cold-start and of 6.524  $\mu\text{W}\cdot\text{cm}^{-2}$  (i.e. -0.54 dBm or 884.2  $\mu\text{W}$  harvested) for the normal charging are required. This corresponds to a maximum range of use of the Wireless Power Transfer system of respectively 3.63 m and 1.56 m. By using a metallic reflector plane, which increases the gain up to + 5.00 dBi, these ranges are increase up to 4.94 m and 2.21 m.

Thus, for the 22 mF supercapacitor, a power density of 0.462  $\mu\text{W}\cdot\text{cm}^{-2}$  (i.e. -12.04 dBm or 62.6  $\mu\text{W}$  harvested) for the cold-start and of 0.667  $\mu\text{W}\cdot\text{cm}^{-2}$  (i.e. -10.45 dBm or 90.2  $\mu\text{W}$  harvested) for the normal charging are required. This corresponds for a maximum range of use of the Wireless Power Transfer system of respectively 5.86 m and 4.88 m. By using a metallic reflector plane, which increases the gain up to + 5.00 dBi, these ranges are increase up to 8.34 m and 6.93 m.

Nevertheless, these results are obviously only very simplified theoretical estimations in the worst case, considering only the unique path through the direct line of sight (no multipath propagation, nor interferences), and for a 10 k $\Omega$  resistive load. In the case of the targeted load (the power management subsystem), because of a variation of its input impedance and more generally of its properties (function of the input and the outputs, such as the voltage in the energy buffer), it is not feasible to obtain in a simple way the efficiency against power densities measurement for the rectenna.

Several improvements in the design can be carried out in order to increase the range of use. First, more efficient components can be used: rectifier with higher efficiency, Power Management Unit requiring less power, and energy buffer with lower losses. Secondly, the energy required by the data management part can be reduced: in that way, the capacitance could be reduced and/or the activation threshold voltage could be decreased, this tends to reduce the maximum losses of the energy buffer. By reducing the required power in the worst case, it becomes possible to use the Sensing Nodes with lower power densities, and thus, on wider ranges. Moreover, the lower the required energy, the faster the charging time, and for equivalent power losses, the lower the energy losses.

#### h. Strategy of Control

The Sensing Nodes are inaccessible once deployed. This inaccessibility is both hardware and software: there is no means to have a physical access (because buried into reinforced concrete) and no mean to have a wireless digital access (because designed without data downlink). Neither the hardware nor the software can be updated or replaced, and also, these must work for long-term. Moreover, the periodicity of functioning is not controlled by the software (e.g., with events or timer interruptions). Even though there are no conventional way to control the Sensing Nodes, their periodicity of functioning can be wirelessly and remotely controlled by the Communicating Nodes through the power downlink achieved by the Wireless Power Transfer. This control can be performed by tuning their wireless power source in terms of waveform, output power and/or periodicity of activation/duty cycle.

To be efficient, this strategy of control must be based on the knowledge of the Communicating Nodes of the energy needs of each Sensing Node located in their neighborhood (in terms of the power required and of the duration of the power supply). For instance, by considering that a unique Communicating Node requires  $H$  hours to wirelessly power all the Sensing Nodes in its neighborhood, and if a measurement is required each  $H$  hours, the Communicating Node can activate continuously its power source. However, if a measurement is required each  $D$  days, it can activate its power source only  $H$  hours each  $D$  days, or reduce the transmission power and adapt the duration (higher than  $H$  hours) at the condition that all the Sensing Nodes can always harvest enough power.

It should be noted that because of the "store then use" strategy, the periodicity of activation of each Sensing Node in the neighborhood of a same Communicating Node is a function of the available electromagnetic power, and thus, it is specific for each Sensing Nodes. Also, this periodicity is a function of: the distance between the Sensing Node and the Communicating Node; the relative orientation and polarization matching between the antennas of the Sensing Node and Communicating Node; the electromagnetic properties of the propagation medium (e.g. metallic rebars position, humidity rate); etc. The temporal characterization of the Sensing Nodes

allows to estimate the time required for the Communicating Node to power or interrogate all the Sensing Node accessible in its neighborhood. The same Sensing Node will transmit several measured data during a specific time slot and thus, it allows the temporal redundancy. As a large majority of Sensing Nodes are accessible during a measurement campaign, a good spatial precision can be obtained. If some Sensing Nodes are non-reachable, the spatial redundancy allows to have enough precision. Finally, the variability in periodicity of activation of the Sensing Nodes is an efficient way to avoid collisions and interferences during data transmissions, which is already limited by the design of the LoRaWAN technology.

To go further, we could consider the case of several fleets of Sensing Nodes, where each fleet is dedicated to the measurement of specific parameters and whose frequency band dedicated to the Wireless Power Transfer does not overlap the bands of the other fleets. Thus, each fleet can be discriminated by the configuration of their Wireless Power Transfer interface, and can be powered independently. In consequence, by tuning both the central frequency and the bandwidth of the generated radiative electromagnetic power by the Communicating Nodes, it becomes possible to power only a part of the fleets of Sensing Nodes, or to provide at each one a different periodicity of functioning.

To increase the end-to-end efficiency, beamforming [62-64] and/or Frequency Diverse Arrays (FDA) [65,66] solutions can be applied in the radiative electromagnetic power source to independently or/and individually power each Sensing Node.

#### i. Implementation of the Sensing Nodes

Several prototypes of Sensing Nodes have been manufactured, as presented in Fig. 11 [16]. These use a unique antenna with a radiofrequency circulator, have a Printed Circuit Board (PCB) embedding the data management and the power management subsystems, and present some interface to connect the different kinds of sensors available on daughter boards. The implemented firmware specifies the unique identifiers, and is a function of the chosen sensor and of the chosen configuration for the wireless communication.

### III. EXPERIMENTAL RESULTS

Several Sensing Nodes have been implemented, tested and characterized [16-18], in particular four in the latest version which are those presented in this Section. Their power consumption versus the configuration of the wireless communication and versus the used sensor, the duration of the first charge and of recharges, the required minimum radiative electromagnetic power as well as the estimated maximum range of use, the reproducibility (study based on all the Sensing Nodes implemented regardless their version), the efficiency, and the test in various configurations are key elements to certify the good functioning of the proposed Sensing Nodes.

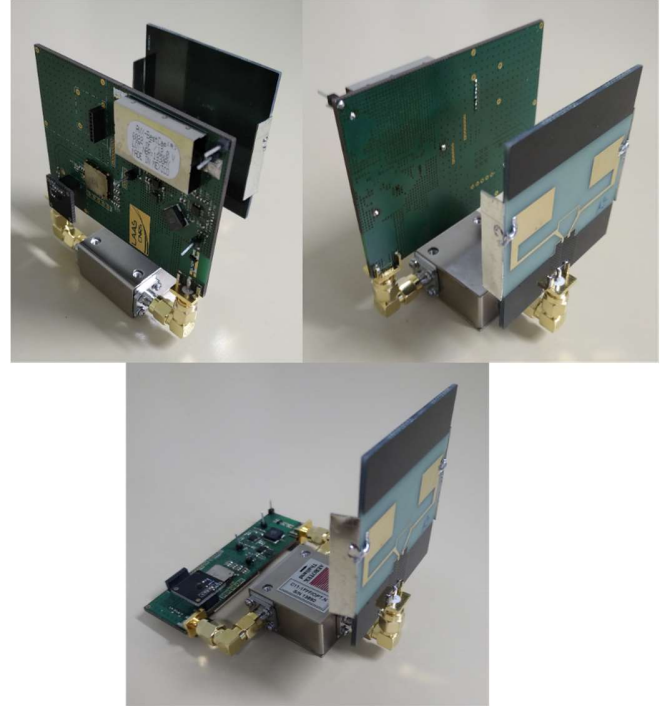


**Fig. 11.** Photographs of prototypes of the sensing nodes, using or not the Printed Circuit Board as a 6 cm x 8 cm metallic reflector plane located at 5 cm below the unique antenna.

#### A. Characterization of the Power Consumption

The power consumption of the data management subsystem constraints the design of the power management subsystem. This power consumption depends on the configuration of the wireless communication (in particular the transmission power, the data-rate (related to the duration of the transmission), and the size of the data payload); and on the sensor used. The objective is to provide the best trade-off between the reliability of the wireless communication and the power consumption. Furthermore, both hardware and software optimizations can still be performed to minimize as much as possible the energy required.

Currently, the LoRaWAN wireless communication technology is employed. Each communication slot is composed of a 17 bytes long LoRaWAN frame, whose 13 bytes are dedicated to the LoRaWAN protocol and 4 bytes dedicated to the data payload. Whatever the sensor used, the data payload could be reduced regarding the quantity of data to send (currently two) and by optimizing the data format (currently each data is formatted on two bytes). By reducing the data payload, it is possible to shorten the wireless transmission and to reduce the energy required for it. Generally, the energy required for the wireless transmission is higher than the energy required for the other processes (initialization, measurement, data formatting, etc.). For all the tested Sensing Nodes, the energy required for their initialization is quite similar (11.3 mJ in average), whatever the configuration of the wireless communication and the sensor used.

### 1. Power Consumption versus Transmission Power

The transmission power is the first parameter of the configuration of the wireless communication which can be optimized. Indeed, the higher the transmission power is, the higher the energy required. Nevertheless, the lower the transmission power is, the shorter the range.

Fig. 12 presents the power consumption of the Sensing Nodes versus the transmission power, for a fixed data-rate of 250 bps (DR0) and 4 bytes of data payload. For this data-rate and this data payload, the data transmission lasts 1318.9 ms. The used LoRa module allows transmission power between +4 dBm and +16 dBm, with a step of +2 dBm. Thus, 160.5 mJ in average (or 40.125 mJ per data byte, or 9.44 mJ per transmitted byte, or 1.18 mJ per transmitted bit) are required for a +14 dBm wireless transmission and 80.6 mJ (or 20.15 mJ per data byte, or 4.74 mJ per transmitted byte, or 0.59 mJ per transmitted bit) in average for a +4 dBm wireless transmission. Therefore, by reducing from +14 dBm to +4 dBm the transmission power, the energy required for the wireless communication is almost halved, and the range of use is always sufficient: at least tens of meters even from a reinforced concrete beam and indoors.

### 2. Power Consumption versus Data-Rate

The data-rate is another parameter of the configuration of the wireless communication which can be optimized. Indeed, the faster the data-rate is, the shorter the duration of the data transmission, and the lower the energy required. Nevertheless, the faster the data-rate, the shorter the range is (because the demodulation becomes more complex).

Fig. 13 presents the power consumption of the Sensing Nodes versus the data-rate, for a fixed power transmission of +4 dBm and for a 17 bytes long LoRaWAN frame. For 4 bytes of data payload, the data transmission lasts 1318.9 ms with the data-rate of 250 bps (DR0) and 51.5 ms with the data-rate of 5470 bps (DR5). Thus, 80.6 mJ (or 20.15 mJ per data byte, or 4.74 mJ per transmitted byte, or 0.59 mJ per transmitted bit) in average are required for a wireless transmission at a data-rate

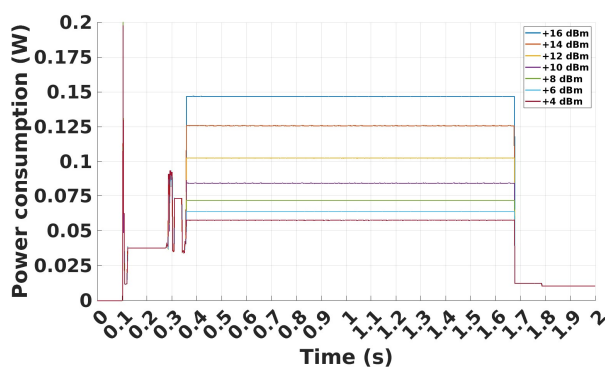


Fig. 12. Power consumption of the Sensing Node against the data transmission power, for the slowest data-rate (DR0) and a 4 bytes data payload.

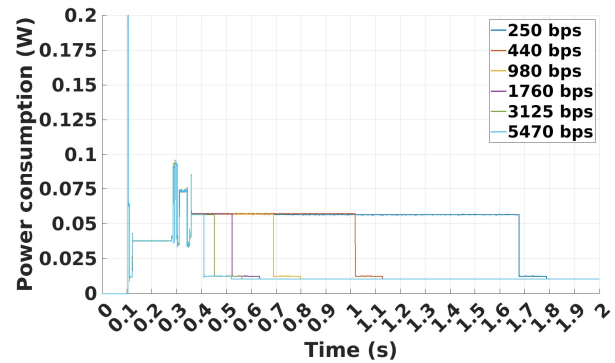


Fig. 13. Power consumption of the Sensing Node against the data-rate, for a +4 dBm transmission power and a 4 bytes data payload.

of 250 bps, and 4.68 mJ in average (or 1.17 mJ per data byte, or 0.28 mJ per transmitted byte, or 34  $\mu$ J per transmitted bit) for a wireless transmission at a data-rate of 5470 bps. Thus, by increasing from 250 bps to 5470 bps the data-rate, the energy required for the wireless communication is almost divided by 17, and the range of use is always sufficient: at least a few tens of meters even from a reinforced concrete beam and indoors. For the fastest data-rate, the energy required for the wireless transmission is lower than the energy required for the other processes (initialization, measurement, data formatting, etc.). In this case, further optimizations -especially in the low-level software- must be achieved to reduce the overall power consumption of the Sensing Nodes.

### 3. Power Consumption versus Sensor

Because the Sensing Nodes are designed in order to be generic platforms where different kinds of sensor can be connected *via* specific daughter boards, the power consumption of each sensor must be limited. Consequently, these must be low power, have similar energy requirements and provide a similar amount of data in order to transmit a LoRaWAN data frame of similar length and duration.

Fig. 14 presents the power consumption of the Sensing Nodes all based on an identical version of the electronic board versus the sensor connected on the board with a specific daughter board and with the associated firmware. The measurements are for a fixed power transmission of +4 dBm, a fixed data-rate of 5470 bps and for a 17 bytes long LoRaWAN frame with 4 bytes of data payload. Thus, the HDC2080 sensor from Texas Instruments (Dallas, Texas, United States of America) requires 0.56 mJ of additional energy, the thermodiodes 3.03 mJ, the strain gauge 4.81 mJ, and the resistivity sensor 3.16 mJ. These additional energies are limited and can be minimized by hardware optimizations, especially on the daughter boards. By considering this diversity, the power management subsystem can be tuned to make the Sensing Nodes generic in terms of the employed sensors. Also, the simultaneous use of multiple sensors must be investigated.

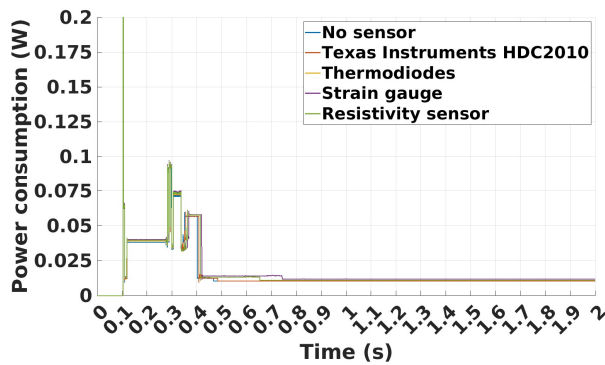


Fig. 14. Power consumption of the Sensing Node against the sensor, for the fastest data-rate (DR5), a 4 bytes data payload, and a +4 dBm transmission power.

#### 4. Overall Power Consumption

Finally, the energy required for a complete process depends on the configuration of the wireless communication (including transmission power and data-rate), and is little influenced by the sensor used. Thus, for the transmission of 4 bytes of data payload in a 17 bytes long LoRaWAN frame, in the worst case for the most reliable configuration of the wireless communication (transmission power of +14 dBm, and data-rate of 250 bps) 210 mJ are required. On the other hand, in the worst case for the less reliable configuration of the wireless communication (transmission power of +4 dBm, and data-rate of 5470 bps), that still meets the requirements, 20 mJ are required. By using the average energy required and by adding 20 % to compensate the variability and the aging, 250 mJ are stored in the first case and 21 mJ in the second. This represents respectively 62.5 mJ of stored energy per data byte (or 14.71 mJ of stored energy per transmitted byte, or 1.84 mJ of stored energy per transmitted bit); and respectively 5.25 mJ of stored energy per data byte (or 309 mJ of stored energy per transmitted byte, or 39  $\mu$ J of stored energy per transmitted bit).

#### B. Temporal Characterization of the Duration of the First Charge and Recharges versus the Available Input Power

The duration of the first charge and recharge gives a good approximation of the shortest periodicity of functioning of the Sensing Nodes possible depending on the available power it can harvest, and thus, indirectly of the distance to the power source(s). The energy to be stored by the power management subsystem and its efficiency constraint the duration of a first charge (from an empty energy buffer) and of recharges (from a previous complete charge). The efficiency is highly impacted by the efficiency of the rectenna, the power required by the Power Management Unit to work, and by the power losses of the DC-to-DC converter and of the energy buffer, the latter are function of the applied voltage. The objective is to provide the most efficient power management subsystem with the fastest charges and the lowest possible required input power to ensure the widest possible ranges. Moreover, hardware optimizations can still be performed in order to

improve as much as possible the efficiency.

#### 1. Duration of the First Charge and Recharges versus the Available Input Power

The characterization presented in Fig. 15 has been performed at 868 MHz, which is within a few MHz of the frequency to get the optimum use of the rectifier, and by applying a conducted electromagnetic power at the input of the radiofrequency circulator to transmit it to the input of the rectifier. The durations are computed by using the timestamps provided by the Communicating Node for each received LoRaWAN frame transmitted by the Sensing Node under test.

Most of the first charges are performed under the cold-start process, during which an input voltage of around 330 mV is imposed by the Power Management Unit, as presented in Fig. 10, which does not allow optimizing the power exchange between the rectenna and the energy buffer. Indeed, the rectifier is more efficient for higher voltages by considering the same input power. Once the cold-start is achieved, thanks to the activation of the hardware Maximum Power Point Tracking system, the power exchange between the rectenna and the energy buffer is improved. It must be noted that the rectifier output voltage saturates for the highest input powers. Generally, the lower the energy to be stored, the faster the charge; and the lower the available input power, the slower the charge.

For the less reliable configuration of the wireless communication (transmission power of +4 dBm, and data-rate of 5470 bps) which requires 21 mJ to be stored, the Sensing Nodes can work with an input down to -17 dBm (or 20.0  $\mu$ W) provided by the antenna to the radiofrequency circulator and at least up to +15 dBm (or 31.6 mW). Thus, the first charge lasts from around 17 hours and 21 minutes, to around 30 seconds, while the recharges from around 7 hours and 59 minutes, to around 6 seconds.

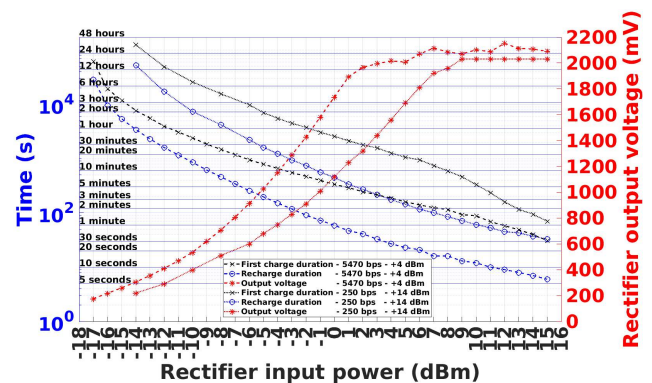


Fig. 15. Durations of the first charge ('x', left) and recharges ('o', left), and rectifier output voltages in open-circuit during the recharges ('\*', right) against the conducted electromagnetic input power applied at the input of the rectifier of the Sensing Nodes, for a frequency of 868 MHz, and for two configurations of the wireless communication: transmission power of +4 dBm and data-rate of 5470 bps (dashed lines), and transmission power of +14 dBm and data-rate of 250 bps (dotted lines).

For the most reliable configuration of the wireless communication (transmission power of +14 dBm, and data-rate of 250 bps) which requires 250 mJ to be stored, the Sensing Nodes can work with an input down to -14 dBm (or 39.8  $\mu$ W) provided by the antenna to the radiofrequency circulator and at least up to +15 dBm (or 31.6 mW). Thus, the first charge lasts from around 34 hours and 36 minutes, to around 1 minute and 10 seconds, while the recharges from around 14 hours and 38 minutes, to around 33 seconds.

Therefore, longer periodicities can be obtained by controlling the duration and periodicity of activation of the power source by the Communication Node(s), and thus, without altering neither the software nor the hardware of the Sensing Nodes.

## 2. Minimum Input Power and Experimental Estimation of the Range of Use

As a reminder, the estimation of the maximum range to operate properly the Sensing Nodes according to the theoretical minimum required input power in function of the employed supercapacitor and in the worst case, are, respectively for the cold-start and the normal charging, for the 2.2 mF capacitance: 3.63 m and 1.56 m with the +1.54 dBi gain antenna, and 4.94 m and 2.21 m with the +5.00 dBi gain antenna; and for the 22 mF capacitance: 5.86 m and 4.88 m with the +1.54 dBi gain antenna, and 8.34 m and 6.93 m with the +5.00 dBi gain antenna. These worst cases have apparently never been met during the various tests and characterization carried out. Indeed, the Sensing Nodes have properly operated for power at the input of the radiofrequency circulator down to -17 dBm (or 20.0  $\mu$ W) and -14 dBm (or 39.8  $\mu$ W), respectively for the less and the most reliable configurations of the wireless communication, both for the cold-start and the normal charging.

Thus, by applying the Friis equation, the distance between a Communicating Node and specifically its Equivalent Isotropic Radiated Power of +33 dBm (or +3 dB, or 2 W) in the 868 MHz Industrial, Scientific and Medical frequency band, and a Sensing Node equipped with the +1.54 dBi gain antenna can be estimated in the function of the required input power obtained experimentally. Thus, -14 dBm (or 39.8  $\mu$ W) can be harvested at a distance of around 7.35 m and -17 dBm (or 20.0  $\mu$ W) at around 10.38 m, and around -10.6 dBm (or 87.1  $\mu$ W) can be harvested at a distance of 5 m. By using a metallic reflector plane to get the +5.00 dBi gain antenna, -14 dBm (or 39.8  $\mu$ W) can be harvested at a distance of around 10.95 m and -17 dBm (or 20.0  $\mu$ W) at around 13.78 m, and around -7.2 dBm (or 190.5  $\mu$ W) can be harvested at a distance of 5 m.

It must be noted that a -17 dBm (or 20.0  $\mu$ W) as minimum power at the output of the antenna is one of the lowest found in the literature. At our best knowledges, only [59] provides a power management subsystem which needs -19 dBm (or 12.5  $\mu$ W) in the 868 MHz Industrial, Scientific and Medical frequency band and -19.5 dBm (or 11.2  $\mu$ W) in the 915 MHz Industrial, Scientific and Medical frequency band.

## C. Study of the Reproducibility

In order to quantify the number of iterations to consider to be able to provide a relevant estimation of the average value from the measured data, few statistical analyses have been carried out.

### 1. Reproducibility for a Sensing Node

First, the variability for each Sensing Node has been measured. Because of the very long time required for the measurements, the study has been limited to two conducted electromagnetic powers at the input of the radiofrequency circulator: +15 dBm (or 31.6 mW) and +0 dBm (or 1.0 mW). Several sets of data have been produced at different times and under different environmental conditions, for Sensing Nodes using a 22 mF supercapacitor. The sets dedicated to the first charges are also limited because of the required time of measurements.

Regarding the duration of the recharges for a power of +15 dBm (or 31.6 mW), the average is closely similar in the various sets and the standard deviation is limited around 3.94 % (or 1 second, that says the measurement step). Hence, the deviations can be mainly explained by the measurement precision (1 second) and by the functioning of the hardware Maximum Power Point Tracking system. Indeed, this achieves a sampling of the input open-circuit voltage each 16 s for nearly 256 ms, and matches its input impedance in the function of the sampled voltage and the voltage in the energy buffer. Depending on the time in the charge when the sampling takes place, (*e.g.*, just after the discharge, just before the discharge, etc.), the impedance matching will be different, and the voltage provided by the rectifier will vary, all that will induce non-negligible time variation for the short recharges.

Regarding the duration of the first charge for a power of +15 dBm (or 31.6 mW), the average is closely similar in the various sets and the standard deviation is limited to 1 second (or 0.88 %), that says the measurement step. Thus, the deviations can be mainly explained by the measurement precision (1 second).

Regarding the duration of the recharges for a power of +0 dBm (or 1.0 mW), the average is closely similar in the various sets and the standard deviation is limited to few seconds, that says around 1.15 %.

Regarding the duration of the first charge for a power of +0 dBm (or 1.0 mW), the average is closely similar in the various sets and the standard deviation is around 2.56 %.

From these observations, it has been decided to consider the average value for at least 10 measurements in order to conserve a relevant order of magnitude.

### 2. Reproducibility Between Sensing Nodes

As presented in Fig. 16 and Fig. 17, there are few variations between the power consumption of different Sensing Nodes. These differences are mainly due to the variability in the components. In consequence, this variability is around 4.2 % and is compensated in the design of the Sensing Nodes by the 20 % overestimation in the quantity of energy to store.

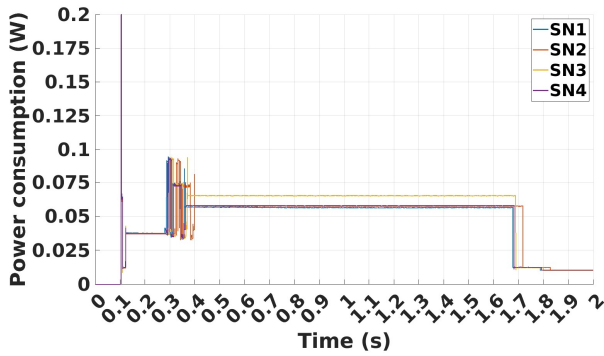


**Fig. 16.** Power consumption of the Sensing Nodes for a transmission power of +14 dBm and the slowest data-rate (DR0).

*D. Study of the Efficiency*

One of the figures of merit of the Sensing Node is the energy efficiency. This is defined here as the ratio of the energy available at the input of the Sensing Node (*i.e.* the power available at the input of the Sensing Node (the one harvested by the antenna) integrated over the period of interest) to the energy required for a complete process. This criterium must be considered in order to provide a sustainable system.

According to Fig. 18, the efficiency is rather low for the first charge: between 2.16 % and 11.54 % for the Sensing Node with the less reliable configuration of the wireless communication and a 2.2 mF supercapacitor; and between 4.59 % and 10.25 % for the Sensing Node with the most reliable configuration of the wireless communication and a 22 mF supercapacitor; and according to Fig. 19, the efficiency is increased for the recharges, respectively: between 3.68 % and 36.71 %; and between 7.91 % and 39.00 %. It must be noted that the two configurations do not present their peak of efficiency for the same input power. These are respectively reached at -9 dBm and at -5 dBm for the first charge, and at -2 dBm and at +1 dBm for the recharges. In addition, the first configuration is more efficient for the lowest input powers, and the second for the highest.

To improve the efficiency of the Sensing Node, the duration of the first charge and recharges must be minimized.

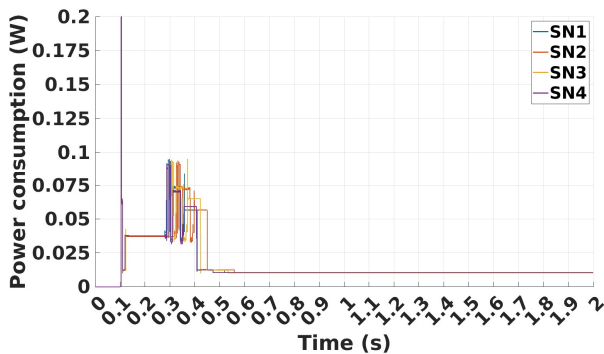


**Fig. 17.** Power consumption of the Sensing Nodes for a transmission power of +4 dBm and the fastest data-rate (DR5).

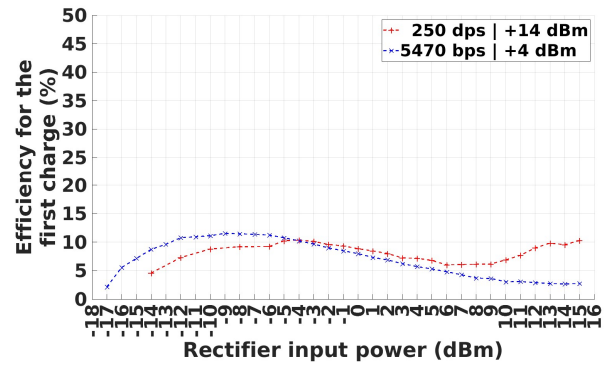


**Fig. 18.** Energy efficiency of the Sensing Nodes during the first charge against the conducted electromagnetic input power applied at the input of the rectifier, for a frequency of 868 MHz, and for two configurations of the wireless communication: transmission power of +4 dBm and data-rate of 5470 bps (blue), and transmission power of +14 dBm and data-rate of 250 bps (red).

Another efficiency which could be relevant to express is the one defined as the ratio of the energy transmitted by a Communicating Node to wirelessly power all the Sensing Nodes located in its neighborhood, to the sum of the energies consumed by each Sensing Node during a period of interest. In this case, the more Sensing Nodes there are, the higher the overall efficiency; and the higher the efficiency of each Sensing Node, the higher the overall efficiency.

*E. Qualitative Results*

To certify the proper functioning of the complete Cyber-Physical System, and of each of its components (namely the Sensing Nodes and the Communicating Nodes) several qualitative tests have been successfully performed, in several configurations.

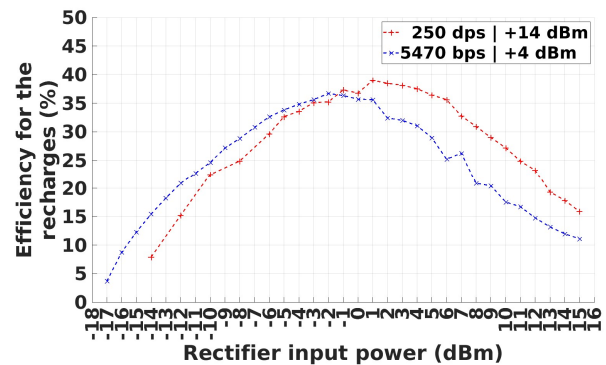


**Fig. 19.** Energy efficiency of the Sensing Nodes during the recharge against the conducted electromagnetic input power applied at the input of the rectifier, for a frequency of 868 MHz, and for two configurations of the wireless communication: transmission power of +4 dBm and data-rate of 5470 bps (blue), and transmission power of +14 dBm and data-rate of 250 bps (red).

For instance, a Cyber-Physical System composed of a meshed network of 2 Communicating Nodes (only 1 with a connection to the Internet) and 4 Sensing Nodes, whose 3 located in the air cavities of a reinforced concrete beam, as partially presented in Fig. 20, have successfully been deployed and tested for temperature, relative humidity and electrical resistivity measurements. In this set-up, a Communicating Node has wirelessly powered and controlled over meters (at least 3 m, with at least 15 cm of reinforced concrete) the Sensing Nodes embedded in the reinforced concrete beam or located close to. It was observed that the 2 Communicating Nodes received all the data sent by the Sensing Nodes over at least a few tens of meters, and processed, stored and shared these in the meshed Network and with the digital world *via* the Internet. Obviously, a unique Communicating Node can easily manage several Sensing Nodes omnidirectionally over several meters.

Moreover, indoors tests have allowed to successfully power and control Sensing Nodes with a unique Communicating Node at a distance of 11 meters in the air, and it seems possible to achieve wider ranges.

Other relevant tests concern the use of the wireless power source in the air cavities of the reinforced concrete beam. With the power source in the central air cavity, it has been possible to power Sensing Nodes located in the two other air cavities, that says, through at least 30 cm of reinforced concrete, but also other Sensing Nodes located outside the reinforced concrete beam and over some meters. Finally, by locating the power source in one of the extremum air cavities and by filling the central air cavity with a reinforced concrete cap, a Sensing Node placed in the other extremum air cavity has been successfully powered, that says through at least 75 cm of reinforced concrete, in the case of a direct line of sight and without external reflection on the floor or wall.

During all the experiments, no LoRaWAN frame transmitted by the Sensing Nodes (with a single or two different antennas)



**Fig. 20.** Photographs of a complete Cyber-Physical System composed of 3 Sensing Nodes embedded in a reinforced concrete beam, and of 1 Communicating Node.

were lost. It should be noticed that the two antennas of the Communicating Nodes (a transmitting antenna for the Wireless Power Transfer, and a receiving antenna for the LoRaWAN data transfer) are located in the same reduced space and operate with the same linear polarization.

In conclusion, the qualitative tests have shown a strong disparity of the obtained results in function of the relative position of the Sensing Nodes with respect to the reinforced concrete and to the Communicating Node(s). They have also shown a very wide disparity in the properties of the reinforced concrete, which highly affects the Wireless Power Transfer [19].

#### IV. DISCUSSION

The objective of this work is to design and implement a Cyber-Physical System based on the use of generic, low-power, fully wireless, fully buried, battery-free, and omnidirectionally, wirelessly and remotely over meters powered and controlled Sensing Nodes, and which is dedicated to the Structural Health Monitoring of reinforced concrete in its full life, *i.e.* for decades.

##### A. Current Solutions for the Structural Health Monitoring of Reinforced Concrete

Among the Smart Concretes as defined in the civil engineering industry [67-69], a major part targets the same objectives as the McBIM project, *i.e.* for the Structural Health Monitoring: this is the self-sensing concretes. These can be intrinsic [68-71] or non-intrinsic (or instrumented by embedding transducers and/or sensors) [68,72-76] self-sensing, but can even be defined as "connected" [77-80].

The current intrinsic [68-71] and non-intrinsic [68,72-76] self-sensing concretes are subjects of laboratory studies, which are not yet able to collect, store or transmit data without the use of an external equipment, generally connected by wires, complex, power consuming, and driven by an operator. Moreover, some of these are based on indirect measurements requiring signal processing, whilst others could be investigated to become transducers for Sensing Nodes.

There are also wireless passive solutions which can be used for traceability or monitoring purposes, and which are based on RadioFrequency Identification (RFID) tags [81-88] or on passive resonators [89,90], buried into concrete. These are not yet able to collect, and then transmit data without the use of a wireless external "reader" usually driven by an operator who must know their location because of the short range of the employed wireless communication technologies based on backscattering. Furthermore, no or only very few amounts of data can be stored.

The other Smart Concretes are the instrumented ones, which are based on Wireless Sensor Networks usually embedded on the surface or buried at a small depth in the concrete (with a maximum depth of 15 cm found in the literature), some are from academics [91-101] and others from industrials [102-112]. Table II. summarizes the properties of the available Sensing Nodes. Most of them use a wireless datalogger or a wireless transmitter manually placed on the surface, and which

TABLE II  
COMPARISON OF CURRENT SENSING NODES FOR THE STRUCTURAL HEALTH MONITORING OF REINFORCED CONCRETE

Ref.	Manufacturer or publication date	Wireless communication technology (frequency)	Deployment strategy (impacting on ease of implementation)	Available sensor(s)	Power source	Estimated lifetime
[77]	Doka	Cellular (2G, 3G, 4G); BLE (2.45 GHz)	Node on concrete surface and sacrificed sensor in concrete	Temperature*	Battery	3 months
[78]	Concrefy	LoRa (868 MHz)	Node on concrete surface	Temperature*; pressure	Battery	N/A
[79]	360 SmartConnect	NFC (13.56 MHz)	Tag a few centimetres in concrete	N/A	Backscattering	Very long
[80]	idencia	RFID (13.56 MHz)	Tag on concrete surface	N/A	Backscattering	Very long
[102]	CAPTAE	Cellular (3G, 4G); RFID (13.56 MHz)	Node on concrete surface	Temperature*; humidity; strength/constraints; elastic and inelastic deformations; inclination; pressure; displacement; defects and shock detection; weather parameters; almost any type of sensor on request	Battery	Between 1 and 3 years
[103]	TELEMAC	Cellular (3G)	Wireless datalogger on concrete surface with 5 wired sacrificed sensors in concrete	Temperature*; humidity; strength/constraints; elastic and inelastic deformations; inclination; load/pressure; displacement; defects and shock detection	Battery	Between 5 and 10 years
[104, 118]	CEMENTYS	LoRa (868 MHz)	Wireless datalogger on concrete surface with 8 wired sacrificed sensors in concrete	Temperature*; humidity; strength/constraints; elastic and inelastic deformations; inclination; load/pressure; resistivity for corrosion estimation	Battery	N/A
[105]	itmsol	Cellular (2G, 3G); BLE (2.45GHz); LoRaWAN (868 MHz); SigFox (868 MHz); NB-IoT; LTE-M; other solutions on request	Wireless datalogger on concrete surface with up to 5 wired sacrificed sensors in concrete	Temperature*; humidity; strength/constraints; elastic and inelastic deformations; inclination; load/pressure; defects and shock detection	Battery	Between 7 months to 6.4 years
[106]	WAKE	Cellular; RFID (13.56 MHz); BLE (2.45 GHz)	Wireless datalogger on concrete surface with up to 24 wired sacrificed sensors in concrete	Temperature*	Battery	Between 4 months and 3 years
[107]	GIATEC	Cellular; Wi-Fi (2.45 GHz); BLE (2.45 GHz)	Node in concrete	Temperature*; strength/constraints	Battery	Up to 4 months
[108]	LumiCON	Cellular	Node in concrete	Temperature*; strength/constraints	Battery	N/A
[109]	HILTI	BLE (2.45 GHz); undefined LPWAN	Node in concrete	Temperature*; strength/constraints	Battery	2 months
[110, 111]	Maturix (Sensohive)	NFC (13.56 MHz); RFID (13.56 MHz); SigFox (868 MHz)	Node on concrete surface and sacrificed sensor in concrete	Temperature*; humidity; strength/constraints	Battery	N/A
[112]	GreenWake Technologies	Non-standardised (868 MHz)	Node on concrete surface	Temperature*; humidity; pressure; acceleration/inclination; magnetic field; luminosity; mechanical deformation	Radiative WPT (2.45 GHz) for battery-free node	Very long
[93]	2009	Non-standardised (2.45 GHz)	Node on concrete surface	Temperature*; humidity; deformations; luminosity; acceleration	Battery	Months
[101]	2009	ZigBee (2.45 GHz)	Node on concrete surface	Impedance	Radiative WPT (2.45 GHz) for battery-free node	Very long
[92]	2011	Non-standardised (433 MHz)	Node in concrete	Temperature*; humidity; impedance	Battery	N/A
[94]	2012	ZigBee (868 MHz)	Node in concrete	Temperature; humidity; electromechanical impedance	Battery	Nearly one month
[115]	2016	LoRa (868 MHz)	Node on concrete surface	Temperature*; humidity; car traffic (indirectly)	Mechanical energy harvesting (vibrations) for battery-free node Inductive WPT (100 kHz) to recharge battery	Long
[97, 98]	2017	Non-standardised (169 MHz)	Node in concrete	Temperature*; strength/constraints	Radiative WPT (845 MHz) for battery-free node	Months
[99]	2018	LoRaWAN (868 MHz)	Node on concrete surface	Temperature*	Solar energy harvesting to recharge battery	Very long
[113]	2018	LoRaWAN (868 MHz)	Node on concrete surface	Crackmeter	Solar energy harvesting to recharge battery	10 years
[114]	2019	LoRaWAN (868 MHz)	Node on concrete surface	Temperature*; humidity; pressure; displacement; acceleration/inclination; magnetic field	Solar energy harvesting to recharge battery	N/A
[119]	2020	Wired (N/A)	Sensor in concrete and pseudo-node on concrete surface	Resistivity for corrosion estimation	External (laptop via USB)	N/A
This work	Since 2018	LoRaWAN (868 MHz)	Node in concrete	Temperature*; humidity; deformations; resistivity for corrosion estimation	Radiative WPT (868 MHz) for battery-free node	Very long

\* Temperature measurements (that can be combined with humidity and/or strength measurements) are usually used during the curing phase in order to monitor the concrete maturity.

N.B.: Cost information for each Sensing Node is not available.

use one or several wired and sacrificed sensors buried in the concrete or placed on its surface. These solutions are increasingly using a wide variety of wireless communication

technologies in order to remotely and digitally store and process the collected data. By removing the wires, the networks become more easily scalable, need less deployment

time, and thus, are less expensive. Regarding the wireless communication, the useful range is between some meters and hundreds of meters. A battery powers all these solutions, and therefore, those of the accessible solutions must periodically recharge or change it, and for the inaccessible solutions their lifetime is limited to a few months or a few years. Among the commercially available solutions, only [112] provides ambient energy harvesting or Wireless Power Transfer solution for powering the Sensing Nodes.

All the current solutions can be deployed for low to medium term periods, often requiring external equipment, and can monitor, between others, the mechanical deformation, the moisture, the temperature, the pH, or the corrosion, but even detect and localize damages.

Moreover, the solutions based of Wireless Sensor Networks allow to connect concrete [91-112]. Another way to achieve this is to use embedded wireless tags (*e.g.*, RFID, NFC, etc.) which provide some information such as an identifier or a Uniform Resource Locator (URL) to wirelessly access through the Internet, the data in relation to the interrogate element [77-80].

Nevertheless, few works deal with the recharge of the battery located in the concrete by the use of an inductive short-range Wireless Power Transfer system [97,98]. Also, few wireless sensors deployed on concrete elements are battery-free and wirelessly powered by a radiative Wireless Power Transfer system [99,101,112]. Finally, few solutions of wireless sensors dedicated to the Structural Health Monitoring of concrete structures use the ambient energy harvesting (from solar energy [113,114] or mechanical vibrations [115]) to recharge batteries and extend their lifetime. However, none of these systems is designed to be buried into concrete to ensure its long-term Structural Health Monitoring, and these are highly dependent on the environment of deployment, of the ambient energy sources and of the targeted application.

Regarding the evaluation of the corrosion, there are no current solutions which are based on low-power, battery-free, fully wireless, and fully buried Sensing Node [24]. Indeed, the commercially available corrosion sensors for the reinforced concretes are usually placed on the surface of the reinforced concrete and have a limited life due to the use of batteries. These are based on the manual measurement of the surface electrical resistivity [116,117]; or are buried in the near surface and are automatically driven by a datalogger [118]. Another solution is based on a passive sensor which can be locally interrogated by a magnetic field [89]. Finally, an electrical resistivity sensor fully buried in reinforced concrete is presented in [119], but this one is not yet able to wirelessly transmit the collected data, and is not energy autonomous. Consequently, to our best knowledge, the first generic Sensing Node dedicated to the Structural Health Monitoring of reinforced concrete, which is fully buried, fully wireless, low-power, battery-free, wirelessly powered and controlled, and part of a Cyber-Physical System that can automate the monitoring, is proposed here.

Thus, the proposed communicating reinforced concrete can be characterized as a non-intrinsic self-sensing and data storing reinforced concrete based on the use of an embedded fully Wireless Sensor Network composed of buried Sensing Nodes employing Non-Destructive Testing methods. These

Sensing Nodes can use a large variety of sensors to measure various parameters of the reinforced concrete during its entire life, and can be considered as wide aggregates planned in the recipe, randomly located and physically inaccessible. The range of use of both the Wireless Power Transfer and the wireless communication of the implemented Wireless Sensor Network covers a relevant volume of reinforced concrete (that says at least from ten of meters in all the directions), and for long-term, (that says for decades). Moreover, its use is automated and does not required human interventions or external equipment; it wirelessly connects the digital world through the Internet; the traceability, the data storage in the material, and the Structural Health Monitoring are simultaneous ensured during all its life. Finally, its deployment is independent of the environment and of the targeted application.

### *B. Current Solutions for the Wireless Power Transfer of Wireless Sensor Networks*

The proposed solution can easily be scalable to other applications and can also be considered as a Wireless Sensor Network wirelessly powered.

Today there are few commercially available solutions to recharge the battery of devices through radiative Wireless Power Transfer [120,121]. Moreover, these are limited in terms of distance and of efficiency: it is more a question of increasing the discharge time of a device than really recharging it during its use.

Nevertheless, some academic researches or few start-up companies deal with complete battery-free Sensing Nodes wirelessly powered through radiative Wireless Power Transfer and which use Low Power Wide Area Networks or Wireless Personal Area Network wireless communication technologies [101,112,122-126]. The latter are compared in Table III. Besides, these meet the requirements of the Simultaneous Wireless Information and Power Transfer paradigm, thanks to frequency and/or spatial multiplexing. Among these, few are dedicated to the Structural Health Monitoring of civil infrastructures but are always deployed on the surface of existing structures and could require the use of a vehicle such as [101,112].

Finally, some works deal with the theoretical or experimental aspects of the radiative Wireless Power Transfer through the reinforced concretes, and study especially the impact of the reinforcements [127-130].

Thus, the proposed solution is only based on off-the-shelf components (excepted for the rectenna, for which no commercial solution is available); employs a unique antenna and a radiofrequency circulator both for the wireless communication and the Wireless Power Transfer which take place in the same Industrial, Scientific and Medical frequency band; allows the implementation of a complete Cyber-Physical System from the measurement inside the reinforced concrete to the process and storage in the digital world *via* the Internet, and through the wireless communication; and is successfully deployed in a harsh environment, namely the reinforced concrete which is a harsh medium of propagation for the electromagnetic waves. Regarding the range of use, this is mainly constrained by the Wireless Power Transfer and not by the wireless communication, but it covers several meters, which is more than

TABLE III  
COMPARISON OF CURRENT SOLUTIONS FOR THE WIRELESS POWER TRANSFER OF WIRELESS SENSOR NETWORKS DEDICATED TO STRUCTURAL HEALTH MONITORING APPLICATIONS

Reference	[101]	[112]	[122]	[126]	[123]	[124]	[125]	Previous version of this work [18]	This work
Date of publication	2009	2021	2017	2019	2021	2017	2018	Since 2018	
Wireless communication technology (frequency)	ZigBee (2.45 GHz)	N/A (N/A)	Bluetooth Low Energy (2.45 GHz)		LoRa (2.45 GHz)	DASH7 (433 MHz)	Bluetooth Low Energy (2.45 GHz)	LoRaWAN (868 MHz)	
Sensor	Impedance	Temperature*; relative humidity; pressure; acceleration; inclination; magnetic field; luminosity; mechanical deformation	Temperature* and relative humidity; acceleration		Acceleration	Temperature* and relative humidity	Temperature*; pressure; acceleration	Temperature* and relative humidity; dielectric resistivity; mechanical deformation	
Wireless Power Transfer frequency	2.45 GHz	2.45 GHz	868 MHz		2.45 GHz	868 MHz	868 MHz	868 MHz	
Transmitted power (dBm)	+30	+27 to +36	+23 to +35	+34.6	+27 (*2)	+27 or +33	+27	+33	
Range of input power (dBm)	N/A	-9 to +15	-10 to +5		N/A	From -17	From -10.5	-14 to +15	-17 to +15
Maximum tested range of use (m)	1	Several meters to few tens of metres (FAQ)	0.5 to 1	1.5	0.54	Up to 8.4 and 16.8 expected	2	7	11
Cold-start compatibility	N/A	N/A	YES		YES	YES	YES	YES	
Periodicity	27 s	N/A	0.5 s		8 s to 259 s	21 s to 2 h 20 min (controlled by MCU)	5 s to 18 s	33 s to 14 h 38 min (controlled by WPT)	6 s to 7 h 59 min (controlled by WPT)
Energy buffer	100 $\mu$ F capacitor	200 $\mu$ F tunable capacitor	Capacitor		2 470 $\mu$ F capacitors	8 mF capacitor	1 mF capacitor	22 mF supercapacitor	2.2 mF supercapacitor
Consumption strategy	Simultaneous store and use	N/A	Simultaneous store and use		Store then use	Simultaneous store and use OR store then use	Store then use	Store then use	
Size (cm x cm x cm)	Not-fully implemented	7 x 5.2 x 0.9 (without antenna)	Not integrated		3 x 3 x 0.5	Not integrated	Not integrated	14 x 9 x 6	8 x 6 x 5

\* Temperature measurements (that can be combined with humidity and/or strength measurements) are usually used during the curing phase in order to monitor the concrete maturity.

a major part of the published solution. Only one proposition provides higher theoretical ranges of use (16.8 meters) but by using a commercially unavailable Power Management Unit [124]. Nevertheless, by optimizing the proposed solution, this range of use seems to be reachable. Because long periodicities are targeted (on a daily, weekly or monthly base) the "store then use" strategy with a cold start ability seems the most appropriate configuration for the targeted application. Furthermore, as long lifespans are wanted, the design provides as little components and complexity as possible in order to limit as much as possible the points of failure.

### C. Areas of Improvement and Future Works

The proposed Sensing Nodes are presented as true prove-of-concept. Nevertheless, these can be optimized both on hardware and on software.

First, each component of the electromagnetic energy harvester (antenna and rectifier), as well as their association (through the impedance matching network), can be improved, and tuned to be the most effective on the targeted frequencies and power densities [5,131]. Moreover, the rectenna can be designed to be multiband or wideband to scavenge a larger part of the available electromagnetic spectrum, and can be placed in arrays to scavenge larger part of the available electromagnetic power. The frequency band(s) and the bandwidth(s) of a rectenna are imposed by the smallest overlap between those of the antenna and those of the rectifier, which is related to their impedance

matching. The relevant parameters of a rectifier are, between others: its topology (*e.g.*, shunt, in series, doubler, Dickson charge pump, etc.); its non-linear rectifying element (*e.g.*, diode, Schottky diode, tunnel diode, metal-insulator-metal diode, spin-diode, complementary metal oxide semi-conductor (CMOS) transistor, etc.); its frequency band(s); and its bandwidth(s). The relevant parameters of an antenna are, between others: its type (*e.g.*, patch, dipole, etc.); its frequency band(s); its bandwidth(s); its polarization (linear, circular or elliptic); its gain in each frequency band(s); and its radiation pattern. Thus, the rectenna can be characterized regarding: its frequency band(s); its bandwidth(s); its minimum power density required; its efficiency; its output voltage and current; its optimal load; but also, its size and its weight. In fact, the size of the Sensing Node is correlated to the size of its antenna, which is closely related to the wavelength, and therefore, a trade-off must be found between volume and performances (especially the radiation pattern and gain). Finally, the rectenna can be manufactured thanks to three-dimensional (3D) or inkjet printing, or additive techniques, and on various substrates (*e.g.*, PolyEthylene Terephthalate (PET), paper, textile, etc.), which can be flexible [5,131].

The antenna must also be tuned to efficiently operate direct contact of the reinforced concrete both for the WPT and the wireless communication [47,52].

In addition to the improvement of the rectenna and with the same aim of lengthening the range of use of the Wireless Power Transfer, the minimum input power required by the data power subsystem must be minimized. This can be achieved by reducing the power required by the Power Management Unit (*e.g.*, by using another one) and lost by the energy buffer and the DC-to-DC converter [57-59].

To shorten the duration of the first charge and recharge, in addition to optimizing the power management subsystem, the energy required by the data management subsystem must be reduced (*e.g.*, by using lower power MicroControler Unit, transceiver, and sensor, or employing other solutions). Thus, first tests have been performed by using Bluetooth Low Energy wireless communication technology (with a QN9080 all-in-one module from NXP Semiconductors (Eindhoven, Netherlands)) rather than LoRaWAN [39]. The implemented Sensing Nodes do not have the same level of maturity as the previous ones and use two antennas because two different Industrial, Scientific and Medical frequency bands are used. The Bluetooth Low Energy is configured in broadcaster/observer mode, and allows to reduce the energy needed by the data management subsystem, at the cost of a less resilient and shorter range wireless communication. This is highly impacted by the reinforced concrete. This implementation requires 1.16 mJ to be stored in a 100  $\mu$ F EEEFK0J101P capacitor from Panasonic (Kadoma, Osaka, Japan). This allows a complete process with the initializations, the measurement, the formatting, and the 4 transmissions of a 19 bytes long advertising frame (whose only 3 bytes are dedicated to the data payload) on 3 different advertising channels for a transmission power of +0 dBm and a data-rate of 1 Mbps. In other words, 1.16 mJ stored is also 390  $\mu$ J per data byte, or 61.6  $\mu$ J per transmitted byte, or 7.7  $\mu$ J per transmitted bit. Consequently, another trade-off between the reliability of the wireless communications and the energy consumption must be sought. The redundancy through the transmission of more

frames on more channels allows to increase the reliability at the cost of more important energy needs.

The current sensors must also be optimized to be more accurate and to consume less power, and other sensors must be employed. In addition, the resistivity sensor must be improved by using an alternative current source to limit the polarization effect on the concrete, and configurations other than the Wenner could be implemented [24,119].

In complement to the improvement of the rectenna, the overall efficiency of the Wireless Power Transfer system and its range of use can be increased by focusing the transmitted power on the Sensing Nodes thanks to beamforming [62-64] or Frequency-Diverse Arrays (FDA) [65,66] techniques, to waste as little power as possible, but also by employing more efficient waveforms [5,64,131,132] or by using relays [133]. Finally, there are also solutions used to recover the energy due to the harmonics lost during the wireless data transmission [134].

With a different approach, alternative strategies of deployment of the Sensing Nodes in the reinforced concrete can be discussed. It is possible: (1) to deploy only the sensor in the core of the concrete and the rest of the Sensing Node near or on the surface so the measurements are performed in the places defined as the most relevant and the Sensing Nodes are accessible, thus replaceable and updatable; but also (2) to deploy the Sensing Node in the core of the concrete and the antenna near or on the surface so the measurements are performed in the places defined as the most relevant and the Sensing Nodes are inaccessible but the constraints of the electromagnetic propagation through the reinforced concrete are released [19]. In these two cases, the use of wires between the different parts can create weaknesses in the reinforced concrete and an access on the surface is also an access point for the pollutants and other contaminants, such as the air and the water which can induce faster corrosion.

A last point of work is the packaging, which must allow to deploy the Sensing Nodes directly in the reinforced concrete (no more in air cavities) and to make possible reliable measurements in it [86,87,94,119,135,136].

Finally, it could be noted that the design and the implementation of this Cyber-Physical System were carried out simultaneously by considering the cyber-security aspects (especially data integrity, confidentiality, and availability), through a security analysis, in particular by defining the main hypothesis of the attacks and its consequences, but also the countermeasures and the security solutions [137].

## V. CONCLUSION

In the framework of the McBIM project, a Cyber-Physical System dedicated to the Structural Health Monitoring of reinforced concrete is proposed through the design and implementation of a communicating reinforced concrete. This industrial Internet of Things system allows to connect the physical and digital worlds through the Internet, by employing a Wireless Sensor Network composed of Communicating Nodes and Sensing Nodes. The Sensing Nodes are able to locally generate, format and transmit measured physical data, and the Communicating Nodes are able to locally gather, locally and/or remotely process, store and exchange the collected data. The Sensing Nodes, which are the core of this paper, are generic being able to use sensors for measuring

various relevant parameters for the Structural Health Monitoring of reinforced concrete (e.g., the temperature, the relative humidity, the mechanical deformation and the electrical resistivity). These are low-power, battery-free, able to cold-start, wirelessly energized and remotely powered and controlled by a radiative Wireless Power Transfer system part of the Communicating Nodes. Moreover, these Sensing Nodes are designed to be fully buried in the reinforced concrete.

The proposed Cyber-Physical System is based on, at our best knowledge, the first fully buried, fully wireless and energy autonomous Sensing Nodes, which is, in addition, able to estimate the corrosion rate by electrical resistivity measurement performed inside the reinforced concrete. This industrial Internet of Things system can be easily scaled to other applications, with less restrictive medium (in terms of electromagnetic waves propagation) than the reinforced concrete. Experimental results demonstrated that the prototypes of the Sensing Nodes have been omnidirectionally powered and controlled by a Communicating Node up to 11 meters indoors. Higher ranges of use (in terms of Wireless Power Transfer) could be achieved with some improvements in terms of rectenna sensitivity and efficiency. It must be noted, that this is not the wireless communications -here based on the LoRaWAN technology (which can work over at least tens of meters from a reinforced concrete beam, and up to kilometers outdoors)- which limits the range of use, but the Wireless Power Transfer, specifically in regards of the maximum Equivalent Isotropic Radiated Power allowed by the regional regulators according to the frequency band (here of +33 dBm, or +3 dB, or 2 W) and the rectenna efficiency. By simultaneously using the 868 MHz Industrial, Scientific and Medical frequency band for both the wireless communication and the Wireless Power Transfer, the Sensing Nodes meet the requirement of the Simultaneous Wireless Information and Power Transfer paradigm by using a unique antenna and a radiofrequency circulator. The Sensing Nodes are considered physically inaccessible because buried in the reinforced concrete, and no data downlink is implemented between the Communicating Nodes and the Sensing Nodes. The periodicity of measurement and wireless communication are not defined by software nor hardware, this is through the Wireless Power Transfer system and its power/energy downlink path that this periodicity is tuned by the Communicating Nodes. Lower the energy to store and higher the power harvested, shorter the periodicity. Thus, a maximum periodicity between several hours and a few seconds can be achieved, respectively for harvested electromagnetic powers (measured at the input of the radiofrequency rectifier) between -17 dBm and +15 dBm.

#### ACKNOWLEDGMENT

The authors would like to thank all their French partners in the McBIM project: CRAN (Nancy, France), LIB (Dijon, France), and FINAO SAS / 360SmartConnect (Trans-en-Provence, France); and in the OPTENLOC project: UWINLOC (Toulouse, France); but also Prof. Jean-Paul Balayssac from the Laboratory for Materials and Durability of Constructions (LMDC, Toulouse, France) and Prof. Florin Udrea, Dr. Andrea De Luca and Dr.

Ethan Gardner from the Centre for Advanced Photonics and Electronics (CAPE) of the University of Cambridge.

#### REFERENCES

- [1] "Machine-to-machine wireless communication technologies for the Internet of Things: Taxonomy, comparison and open issues," *Pervasive and Mobile Computing*, vol. 50, pp. 56-81, 2018.
- [2] S. Zeadally, and N. Jabeur, *Cyber-physical system design with sensor networking technologies*, 1<sup>st</sup> ed., London, United-Kingdom: Institution of Engineering and Technology, 2016, p. 368.
- [3] A. Čolaković, and M. Hadžialić, "Internet of Things (IoT): A review of enabling technologies, challenges, and open research issues," *Computer networks*, vol. 144, pp. 17-39, 2018.
- [4] G. Peruzzi, and A. Pozzebon, "A review of energy harvesting techniques for Low Power Wide Area Networks (LPWANs)," *Energies*, vol. 13, no. 13, p. 3433, 2020.
- [5] A. Georgiadis, A. Collado, and M. M. Tentzeris, *Energy Harvesting: Technologies, Systems, and Challenges*, 1<sup>st</sup> ed., Cambridge, United-Kingdom: Cambridge University Press, 2021, p. 208.
- [6] European Union, COMMISSION IMPLEMENTING DECISION (EU) 2017/1483 of 8 August 2017 amending Decision 2006/771/EC on harmonisation of the radio spectrum for use by short-range devices and repealing Decision 2006/804/EC, *Official Journal of the European Union, Decision C(2017) 5464*, 2017.
- [7] T. D. Ponnimbaduge Perera, D. N. K. Jayakody, S. K. Sharma, S. Chatzinotas, and J. Li, "Simultaneous wireless information and power transfer (SWIPT): Recent advances and future challenges," *IEEE Communication Surveys Tutorials*, vol. 20, no. 1, pp. 264-302, 2018.
- [8] C. R. Farrar, and K. Worden, "An introduction to structural health monitoring," *Philosophical Transactions of the Royal Society A: Mathematical, Physical and Engineering Sciences*, vol. 365, no. 1851, pp. 303-315, 2007.
- [9] J. H. Bungey, S. G. Millard, and M. G. Grantham, *Testing of concrete in structures*, 4<sup>th</sup> ed, Boca Taron, Florida, United States of America: Crc Press, 2006, p. 353.
- [10] S. K. Verma, S. S. Bhadauria, and S. Akhtar, "Review of nondestructive testing methods for condition monitoring of concrete structures," *Journal of construction engineering*, vol. 2013, no. 2008, pp. 1-11, 2013.
- [11] P. Kot, M. Muradov, M. Gkantou, G. S. Kamaris, K. Hashim, and D. Yeboah, "Recent advancements in non-destructive testing techniques for structural health monitoring," *Applied Sciences*, vol. 11, no. 6, p. 2750, 2021.
- [12] S. Tang, D. R. Shelden, C. M. Eastman, P. Pishdad-Bozorgi, and X. Gao, "A review of building information modeling (BIM) and the internet of things (IoT) devices integration: Present status and future trends," *Automation in Construction*, vol. 101, pp. 127-139, 2019.
- [13] S. Kubler, W. Derigent, A. Thomas, and E. Rondeau, "Problem definition methodology for the "Communicating Material" paradigm," *IFAC Proceedings Volumes*, vol. 43, no. 4, pp. 198-203, 2010.
- [14] *McBIM*. Accessed: Apr. 20, 2023. [Online]. Available: <https://mcbim.cran.univ-lorraine.fr/>
- [15] W. Derigent, M. David, H. Wan, D. Dragomirescu, A. Takacs, G. Loubet, A. Roxin, R. Melet, and L. Montegut, "Materials communicating with the BIM: results of the McBIM project," *IFAC-PapersOnLine*, vol. 55, no. 8, pp. 25-30, in 6<sup>th</sup> IFAC Symposium on Telematics Applications TA 2022, Nancy, France, 2022.
- [16] G. Loubet, "Autonomous wireless sensor networks for the implementation of communicating materials. Application to civil engineering industry.," Ph.D. dissertation, INSA Toulouse, Toulouse, France, 24 September 2021.
- [17] G. Loubet, A. Takacs, E. Gardner, A. De Luca, F. Udrea, and D. Dragomirescu, "LoRaWAN Battery-Free Wireless Sensors Network Designed for Structural Health Monitoring in the Construction Domain," *Sensors*, vol. 19, no. 7, p. 1510, 2019.
- [18] G. Loubet, A. Takacs, and D. Dragomirescu, "Implementation of a Wireless Sensor Network Designed to be Embedded in Reinforced Concrete," in *IECON 2020 The 46th Annual Conference of the IEEE Industrial Electronics Society*, pp. 2195-2200, 2020.
- [19] S. S. Zhekov, O. Franek, and G. F. Pedersen, "Dielectric properties of common building materials for ultrawideband propagation studies [Measurements Corner]," *IEEE Antennas and Propagation Magazine*, vol. 62, no. 1, pp. 72-81, 2020.

- [20] S. Taheri, "A review on five key sensors for monitoring of concrete structures," *Construction and Building Materials*, vol. 204, pp. 492-509, 2019.
- [21] A. De Luca, V. Pathirana, S. Z. Ali, D. Dragomirescu, and F. Udreu, "Experimental, analytical and numerical investigation of non-linearity of SOI diode temperature sensors at extreme temperatures," *Sensors and Actuators A: Physical*, vol. 222, pp. 31-38, 2015.
- [22] *Texas Instruments - HDC2010 Low-Power Humidity and Temperature Digital Sensors*. Accessed: Apr. 20, 2023. [Online]. Available: <https://www.ti.com/lit/ds/symlink/hdc2010.pdf>
- [23] *RS Pro - Datasheet RS Pro Wire Lead Strain Gauge 4mm, 120Ω*. Accessed: Apr. 20, 2023. [Online]. Available: <https://docs.rs-online.com/1c95/0900766b815882e1.pdf>
- [24] J. Badr, "Conception et validation d'un capteur noyé de résistance électrique en vue du suivi des profils de teneur en eau dans les bétons," Ph.D. Dissertation, Université Paul Sabatier-Toulouse III, Toulouse, France, 2019.
- [25] IEEE 802.15.7 Working Group. IEEE Standard for information technology - Telecommunications and information exchange between systems - Local and metropolitan area networks - Specific requirements - Part 15.7: Short-range wireless optical communication using visible light. IEEE Standard 802.15.7, 2011.
- [26] S. Siu, Q. Ji, W. Wu, G. Song, and Z. Ding, "Stress wave communication in concrete: I. Characterization of a smart aggregate based concrete channel," *Smart materials and structures*, vol. 23, no. 12, p. 125030, 2014.
- [27] S. Siu, Q. Ji, X. Wu, G. Song, and Z. Ding, "Stress wave communication in concrete: II. Evaluation of low voltage concrete stress wave communications utilizing spectrally efficient modulation schemes with PZT transducers," *Smart materials and structures*, vol. 23, no. 12, p. 125031, 2014.
- [28] G. Saulnier, H. Scarton, D. Shoudy, P. Das, and A. Gavens, "Ultrasonic Through-Wall Communication (UTWC) System," *U.S. Patent Application No. 12/443,878*, 2010.
- [29] J. S. Lee, Y. W. Su, and C. C. Shen, "A comparative study of wireless protocols: Bluetooth, UWB, ZigBee, and Wi-Fi," in *IECON 2007 The 33rd Annual Conference of the IEEE Industrial Electronics Society*, pp. 46-51, 2007.
- [30] IEEE 802.15.1 Working Group. IEEE Standard for information technology - Telecommunications and information exchange between systems - Local and metropolitan area networks - Specific requirements - Part 15.1: Wireless Medium Access Control (MAC) and Physical layer (PHY) specifications for Wireless Personal Area Networks (WPANs). IEEE Standard 802.15.1, 2005.
- [31] IEEE 802.15.4 Working Group. IEEE Standard for information technology - Telecommunications and information exchange between systems - Local and metropolitan area networks - Specific requirements - Part 15.4: Wireless Medium Access Control (MAC) and Physical layer (PHY) specifications for low-rate Wireless Personal Area Networks (WPANs). IEEE Standard 802.15.4, 2006.
- [32] IEEE 802.15.4 Working Group. IEEE Standard for local and metropolitan area networks - Part 15.4: Low-rate Wireless Personal Area Networks (LR-WPANs). IEEE Standard 802.15.4, 2011.
- [33] U. Raza, P. Kulkarni, and M. Sooriyabandara, "Low power wide area networks: An overview," *IEEE Communications Surveys & Tutorials*, vol. 19, no. 2, pp. 855-873, 2017.
- [34] LoRa Alliance Technical Committee. LoRaWAN 1.0.3 specification. 2018.
- [35] International Organization for Standardization/International Electrotechnical Commission. Information technology - Radio frequency identification for item management. ISO/IEC 18000, 2015.
- [36] IEEE 802.15.3 Working Group. IEEE Standard for information technology - Telecommunications and information exchange between systems - Local and metropolitan area networks - Specific requirements - Part 15.3: Wireless Medium Access Control (MAC) and Physical layer (PHY) specifications for high rate Wireless Personal Area Networks (WPAN). IEEE Standard 802.15.3, 2003.
- [37] IEEE 802.15.3 Working Group. IEEE Standard for high data-rate wireless multimedia networks. IEEE Standard 802.15.3, 2016.
- [38] IEEE 1902.1 Working Group. IEEE Standard for long wavelength wireless network protocol. IEEE Standard 1902.1, 2009.
- [39] A. Sidibe, G. Loubet, A. Takacs, and D. Dragomirescu, "A Multifunctional Battery-Free Bluetooth Low Energy Wireless Sensor Node Remotely Powered by Electromagnetic Wireless Power Transfer in Far-Field," *Sensors*, vol. 22, no. 11, p. 4054, 2022.
- [40] *Murata - Sub-G Module Data Sheet*. Accessed: Apr. 20, 2023. [Online]. Available: [https://wireless.murata.com/pub/RFM/data/type\\_abz.pdf](https://wireless.murata.com/pub/RFM/data/type_abz.pdf)
- [41] *Semtech. LoRa—SX1276/77/78/79*. Accessed: Apr. 20, 2023. [Online]. Available: <https://www.semtech.com/products/wireless-rf/lora-transceivers/SX1276>
- [42] *STMicroelectronics. B-L072Z-LRWAN1*. Accessed: Apr. 20, 2023. [Online]. Available: <https://www.st.com/en/evaluation-tools/b-l072z-lrwan1.html>
- [43] J. W. Matiko, N. J. Grabham, S. P. Beeby, and M. J. Tudor, "Review of the application of energy harvesting in buildings," *Measurement Science and Technology*, vol. 25, no. 1, p. 012002, 2013.
- [44] X. Gu, L. Grauwlin, D. Dousset, S. Hemour, and K. Wu, "Dynamic Ambient RF Energy Density Measurements of Montreal for Battery-Free IoT Sensor Network Planning," *IEEE Internet of Things Journal*, vol. 8, no. 17, pp. 13209-13221, 2021.
- [45] *Aeroteck Co., LTD. - Coaxial circulators/isolators*. Accessed: Apr. 20, 2023. [Online]. Available: <http://www.aeroteck.co.th/classic/coaxstd.php>
- [46] A. Sidibe, A. Takacs, G. Loubet, and D. Dragomirescu, "Compact Antenna in 3D Configuration for Rectenna Wireless power transfer Applications," *Sensors*, vol. 21, no. 9, p. 3193, 2021.
- [47] K. M. Shams, M. Ali, and A. M. Miah, "Characteristics of an embedded microstrip patch antenna for wireless infrastructure health monitoring," *IEEE Antennas and Propagation Society International Symposium*, pp. 3643-3646, 2006.
- [48] M. F. Rad, and L. Shafai, "Embedded microstrip patch antenna for structural health monitoring applications," *IEEE Antennas and Propagation Society International Symposium*, pp. 1-4, 2008.
- [49] X. Jin, and M. Ali, "Embedded antennas in dry and saturated concrete for application in wireless sensors," *Progress in electromagnetics research*, vol. 102, pp. 197-211, 2012.
- [50] S. H. Jeong, and H. W. Son, "UHF RFID tag antenna for embedded use in a concrete floor," *IEEE Antennas and Wireless Propagation Letters*, vol. 10, pp. 1158-1161, 2011.
- [51] R. Salama, and S. Kharkovsky, "An embeddable microwave patch antenna module for civil engineering applications," in *I2MTC IEEE International Instrumentation and Measurement Technology Conference*, pp. 27-30, 2013.
- [52] G. Castorina, L. Di Donato, A. F. Morabito, T. Isernia, and G. Sorbello, "Analysis and design of a concrete embedded antenna for wireless monitoring applications [antenna applications corner]," *IEEE Antennas and Propagation Magazine*, vol. 58, no. 6, pp. 76-93, 2016.
- [53] A. Sidibe, G. Loubet, A. Takacs, and D. Dragomirescu, "Energy Harvesting for Battery-Free Wireless Sensors Network Embedded in a Reinforced Concrete Beam," in *EuMC The 50th European Microwave Conference*, pp. 702-705, 2021.
- [54] *Skyworks - Surface-mount mixer and detector Schottky diodes*. Accessed: Apr. 20, 2023. [Online]. Available: [https://www.skyworksinc.com/-/media/SkyWorks/Documents/Products/201-300/Surface\\_Mount\\_Schottky\\_Diodes\\_200041AG.pdf](https://www.skyworksinc.com/-/media/SkyWorks/Documents/Products/201-300/Surface_Mount_Schottky_Diodes_200041AG.pdf)
- [55] *Texas Instruments - BQ25504*. Accessed: Apr. 20, 2023. [Online]. Available: <https://www.ti.com/product/BQ25504>
- [56] *Texas Instruments - TPS6303x High Efficiency Single Inductor Buck-Boost Converter*. Accessed: Apr. 20, 2023. [Online]. Available: <https://www.ti.com/lit/ds/symlink/tps63030.pdf>
- [57] *Texas Instruments - BQ25505*. Accessed: Apr. 20, 2023. [Online]. Available: <https://www.ti.com/product/BQ25505>
- [58] *Texas Instruments - BQ225570*. Accessed: Apr. 20, 2023. [Online]. Available: <https://www.ti.com/product/BQ225570>
- [59] *e-peas semiconductors - AEM30940 - datasheet*. Accessed: Apr. 20, 2023. [Online]. Available: <https://e-peas.com/wp-content/uploads/2021/03/e-peas-AEM30940-datasheet-RF-Vibration-energy-harvesting.pdf>
- [60] *AVX - BestCap*. Accessed: Apr. 20, 2023. [Online]. Available: <https://catalogs.avx.com/BestCap.pdf>
- [61] *Panasonic - Aluminum Electrolytic Capacitor*. Accessed: Apr. 20, 2023. [Online]. Available: <https://industrial.panasonic.com/cdbs/www-data/pdf/RDE0000/ABA0000C1190.pdf>
- [62] D. Belo, D. C. Ribeiro, P. Pinho, and N. B. Carvalho, "A selective, tracking, and power adaptive far-field wireless power transfer system," *IEEE Transactions on Microwave Theory and Techniques*, vol. 67, no. 9, pp. 3856-3866, 2019.
- [63] D. Masotti, M. Shanawani, and A. Costanzo, "Smart Beamforming Techniques for "On Demand" WPT," *Wireless Power Transmission for Sustainable Electronics*, pp. 57-84, 2020.

- [64] J. Kim, and B. Clerckx, "Range expansion for wireless power transfer using joint beamforming and waveform architecture: An experimental study in indoor environment," *IEEE Wireless Communications Letters*, vol. 10, no. 6, pp. 1237-1241, 2021.
- [65] W. Q. Wang, "Retrodirective frequency diverse array focusing for wireless information and power transfer," *IEEE Journal on Selected Areas in Communications*, vol. 37, no. 1, pp. 61-73, 2018.
- [66] E. Fazzini, A. Costanzo, and D. Masotti, "Range Selective Power Focusing with Time-controlled Bi-dimensional Frequency Diverse Arrays," In *WPTC IEEE Wireless Power Transfer Conference*, pp. 1-4, 2021.
- [67] S. Kamila, "Introduction, classification and applications of smart materials: an overview," *American Journal of Applied Sciences*, vol. 10, no. 8, p. 876, 2013.
- [68] B. Han, L. Zhang, and J. Ou, *Smart and multifunctional concrete toward sustainable infrastructures*. Singapore: Springer, 2017, p. 409.
- [69] N. Makul, "Advanced smart concrete-A review of current progress, benefits and challenges," *Journal of Cleaner Production*, p. 122899, 2020.
- [70] B. Han, S. Ding, and X. Yu, "Intrinsic self-sensing concrete and structures: A review," *Measurement*, vol. 59, pp. 110-128, 2015.
- [71] Z. Tian, Y. Li, J. Zheng, and S. Wang, "A state-of-the-art on self-sensing concrete: Materials, fabrication and properties," *Composites Part B: Engineering*, vol. 177, p. 107437, 2019.
- [72] G. Kaklauskas, A. Sokolov, R. Ramanauskas, and R. Jakubovskis, "Reinforcement strains in reinforced concrete tensile members recorded by strain gauges and FBG sensors: experimental and numerical analysis," *Sensors*, vol. 19, no. 1, p. 200, 2019.
- [73] A. Deraemaeker, and C. Dumoulin, "Embedding ultrasonic transducers in concrete: A lifelong monitoring technology," *Construction and Building Materials*, vol. 194, pp. 42-50, 2019.
- [74] G. Song, Y. L. Mo, K. Otero, and H. Gu, "Health monitoring and rehabilitation of a concrete structure using intelligent materials," *Smart materials and structures*, vol. 15, no. 2, p. 309, 2006.
- [75] N. Muto, Y. Arai, S. G. Shin, H. Matsubara, H. Yanagida, M. Sugita, and T. Nakatsuji, "Hybrid composites with self-diagnosing function for preventing fatal fracture," *Composites Science and Technology*, vol. 61, no. 6, pp. 875-883, 2001.
- [76] A. Downey, A. D'Alessandro, F. Ubertini, and S. Laflamme, "Automated crack detection in conductive smart-concrete structures using a resistor mesh model," *Measurement Science and Technology*, vol. 29, no. 3, p. 035107, 2018.
- [77] *Doka*. Accessed: Apr. 20, 2023. [Online]. Available: <https://www.doka.com/>
- [78] *Concrefy*. Accessed: Apr. 20, 2023. [Online]. Available: <https://www.concrefy.com/>
- [79] *360 SmartConnect*. Accessed: Apr. 20, 2023. [Online]. Available: <https://www.360sc.io/?lang=en>
- [80] *idencia - connected concrete*. Accessed: Apr. 20, 2023. [Online]. Available: <http://www.idencia.com/connected-concrete>
- [81] J. Zhang, G. Y. Tian, A. M. Marindra, A. I. Sunny, and A. B. Zhao, "A review of passive RFID tag antenna-based sensors and systems for structural health monitoring applications," *Sensors*, vol. 17, no. 2, p. 265, 2017.
- [82] Build E.R.A. "Review of current state of radio frequency identification (RFID) technology, its use and potential future use in construction", 2006.
- [83] N. Li, and B. Becerik-Gerber, "Life-cycle approach for implementing RFID technology in construction: Learning from academic and industry use cases," *Journal of Construction Engineering and Management*, vol. 137, no. 12, pp. 1089-1098, 2011.
- [84] J. Ikonen, A. Knutas, H. Hämäläinen, M. Ihonen, J. Porras, and T. Kallonen, "Use of embedded RFID tags in concrete element supply chains," *Journal of Information Technology in Construction (ITCon)*, vol. 18, no. 7, pp. 119-147, 2013.
- [85] E. Valero, and A. Adán, "Integration of RFID with other technologies in construction," *Measurement*, vol. 94, pp. 614-620, 2016.
- [86] S. Johann, C. Strangfeld, M. Müller, B. Mieller, and M. Bartholmai, "RFID sensor systems embedded in concrete—requirements for long-term operation," *Materials Today: Proceedings*, vol. 4, no. 5, pp. 5827-5832, 2017.
- [87] S. G. N. Murthy, "Batteryless Wireless RFID based embedded sensors for long term monitoring of reinforced concrete structures," in *International Symposium Non-Destructive Testing in Civil Engineering (NDT-CE)*, pp. 15-17, 2015.
- [88] X. Yi, C. Cho, J. Cooper, Y. Wang, M. M. Tentzeris, and R.T. Leon, "Passive wireless antenna sensor for strain and crack sensing - Electromagnetic modeling, simulation, and testing," *Smart Materials and Structures*, vol. 2, 2013.
- [89] M. M. Andringa, D. P. Neikirk, N. P. Dickerson, and S. L. Wood, "Unpowered wireless corrosion sensor for steel reinforced concrete," *SENSORS*, p. 4, 2005.
- [90] B. Ozbey, V. B. Erturk, H. V. Demir, A. Altintas, and O. Kurc, "A wireless passive sensing system for displacement/strain measurement in reinforced concrete members," *Sensors*, vol. 16, no. 4, p. 496, 2016.
- [91] B. L. Grisso, L. A. Martin, and D. J. Inman, "A wireless active sensing system for impedance-based structural health monitoring," in *IMAC XXIII The 23rd International Modal Analysis Conference*, 2005.
- [92] W. Quinn, P. Angove, J. Buckley, J. Barrett, and G. Kelly, "Design and performance analysis of an embedded wireless sensor for monitoring concrete curing and structural health," *Journal of Civil Structural Health Monitoring*, vol. 1, no. 1, pp. 47-59, 2011.
- [93] M. Ceriotti, L. Mottola, G. P. Picco, A. L. Murphy, S. Guna, M. Corra, M. Pozzi, D. Zonta, and P. Zanon, "Monitoring heritage buildings with wireless sensor networks: The Torre Aquila deployment," in *International Conference on Information Processing in Sensor Networks*, pp. 277-288, 2009.
- [94] C. Y. Chang, and S. S. Hung, "Implementing RFIC and sensor technology to measure temperature and humidity inside concrete structures," *Construction and Building Materials*, vol. 26, no. 1, pp. 628-637, 2012.
- [95] A. B. Noel, A. Abdaoui, T. Elfouly, M. H. Ahmed, A. Badawy, and M. S. Shehata, "Structural health monitoring using wireless sensor networks: A comprehensive survey," *IEEE Communications Surveys & Tutorials*, vol. 19, no. 3, pp. 1403-1423, 2017.
- [96] M. Z. A. Bhuiyan, J. Wu, G. Wang, J. Cao, W. Jiang, and M. Atiquzzaman, "Towards cyber-physical systems design for structural health monitoring: Hurdles and opportunities," *ACM Transactions on Cyber-Physical Systems*, vol. 1, no. 4, pp. 1-26, 2017.
- [97] L. Gallucci, C. Menna, L. Angrisani, D. Asprone, R. S. L. Moriello, F. Bonavolontà, and F. Fabbrocino, "An embedded wireless sensor network with wireless power transfer capability for the structural health monitoring of reinforced concrete structures," *Sensors*, vol. 17, no. 11, p. 2566, 2017.
- [98] L. Angrisani, R. S. L. Moriello, F. Bonavolontà, L. Gallucci, C. Menna, D. Asprone, and F. Fabbrocino, "An innovative embedded wireless sensor network system for the structural health monitoring of RC structures," in *RTSI The 3rd IEEE International Forum on Research and Technologies for Society and Industry*, pp. 1-4, 2017.
- [99] D. Bosma, and P. Lindeman, "Autonomous battery less sensor for IoT applications in Smart Buildings: Low-power Energy Conversion and Storage for RF Energy Harvesting," B.S. Thesis, Delft University of Technology: Delft, Netherlands, 2018.
- [100] M. Abdulkarem, K. Samsudin, F. Z. Rokhani, and M.F. A. Rasid, "Wireless sensor network for structural health monitoring: A contemporary review of technologies, challenges, and future direction," *Structural Health Monitoring*, vol. 19, no. 3, pp. 693-735, 2020.
- [101] K. M. Farinholt, G. Park, and C. R. Farrar, "RF energy transmission for a low-power wireless impedance sensor node," *IEEE Sensors Journal*, vol. 9, no. 7, pp. 793-800, 2009.
- [102] *CAPTAE et le monitoring des structures* Accessed: Apr. 20, 2023. [Online]. Available: <https://lerm.fr/instruments/captae/captae/>
- [103] *TELEMAC - Leading Supplier of Geotechnical & Structural Instrumentation*. Accessed: Apr. 20, 2023. [Online]. Available: <https://telemac.fr/en/>
- [104] *CEMENTYS - Surveillance vos infrastructures*. Accessed: Apr. 20, 2023. [Online]. Available: <https://cementys.com/fr/>
- [105] *itmsol instrumentation & monitoring*. Accessed Apr. 20, 2023. [Online]. Available: <https://www.itmsol.fr/>
- [106] *WAKE - powerful wireless concrete temperature monitoring and reporting*. Accessed: Apr. 20, 2023. [Online]. Available: <https://www.wakeinc.com/>
- [107] *GIATEC - Revolutionizing Concrete Testing*. Accessed: Apr. 20, 2023. [Online]. Available: <https://www.giatecscientific.com/>
- [108] *LumiCON - Concrete sensors*. Accessed: Apr. 20, 2023. [Online]. Available: <https://lumicon.io/concrete-sensors/>
- [109] *HILTI - Concrete sensors*. Accessed: Apr. 20, 2023. [Online]. Available: <https://www.hilti.com/content/hilti/W1/US/en/services/tool-services/internet-of-things/concrete-sensors.html>

- [110] *Sensohive - Wireless sensors and IoT solutions*. Accessed: Apr. 20, 2023. [Online]. Available: <https://sensohive.com/>
- [111] *Maturix*. Accessed: Apr. 20, 2023. [Online]. Available: <https://maturix.com/>
- [112] *GreenWake Technologies - Remote powering of sensors - no wires, no batteries, no worries*. Accessed: Apr. 20, 2023. [Online]. Available: <http://gnw-tech.com/home.htm>
- [113] T. Polonelli, D. Brunelli, M. Guermandi, and L. Benini, "An accurate low-cost Crackmeter with LoRaWAN communication and energy harvesting capability," in *ETFA The 23rd IEEE International Conference on Emerging Technologies and Factory Automation*, vol. 1, pp. 671-676, 2018.
- [114] P. Boccadoro, B. Montaruli, and L. A. Grieco, "Quakesense, a LoRa-compliant earthquake monitoring open system," in *DS-RT The 23rd IEEE/ACM International Symposium on Distributed Simulation and Real Time Applications*, pp. 1-8, 2019.
- [115] F. Orfei, C. B. Mezzetti, and F. Cottone, "Vibrations powered LoRa sensor: An electromechanical energy harvester working on a real bridge," *IEEE SENSORS*, pp. 1-3, 2016.
- [116] *GIATEC - iCOR Wireless NDT Corrosion Detection*. Accessed: Apr. 20, 2023. [Online]. Available: <https://www.giatecscientific.com/products/concrete-ndt-devices/icor-rebar-corrosion-rate/>
- [117] *Screening Eagle - Proceq Resipod*. Accessed: Apr. 20, 2023. [Online]. Available: <https://www.screeningeagle.com/en/products/resipod>
- [118] *CEMENTYS - CorroVolta Corrosion sensor*. Accessed: Apr. 20, 2023. [Online]. Available: <https://cementys.com/en/corrosion-sensor-monitoring-corrovolta/>
- [119] D. M. Corva, S. S. Hosseini, F. Collins, S. D. Adams, W. P. Gates, and A. Z. Kouzani, "Miniature resistance measurement device for structural health monitoring of reinforced concrete infrastructure," *Sensors*, vol. 20, no. 15, p. 4313, 2020.
- [120] *Powercast - Wireless power for a wireless world*. Accessed: Apr. 20, 2023. [Online]. Available: <https://www.powercastco.com/>
- [121] *Ossia*. Accessed: Apr. 20, 2023. [Online]. Available: <https://www.ossia.com/>
- [122] J. Janhunen, K. Mikhaylov, and J. Petäjälä, "Experimental RF-signal based wireless energy transmission," in *EuCNC The IEEE European Conference on Networks and Communications*, pp. 1-6, 2017.
- [123] G. Paolini, D. Masotti, M. Guermandi, M. Shanawani, L. Benini, and A. Costanzo, "An Ambient-Insensitive Battery-Less Wireless Node for Simultaneous Powering and Communication," in *EuMC The 50th IEEE European Microwave Conference*, pp. 522-525, 2021.
- [124] M. Pizzotti, L. Perilli, M. Del Prete, D. Fabbri, R. Canegallo, M. Dini, D. Masotti, A. Costanzo, E. Franchi Scarselli, and A. Romani, "A long-distance RF-powered sensor node with adaptive power management for IoT applications," *Sensors*, vol. 17, no. 8, p. 1732, 2017.
- [125] R. La Rosa, C. Trigona, G. Zoppi, C. A. Di Carlo, L. Di Donato, and G. Sorbello, "RF energy scavenger for battery-free Wireless Sensor Nodes," in *I2MTC The IEEE International Instrumentation and Measurement Technology Conference*, pp. 1-5, 2018.
- [126] J. Janhunen, K. Mikhaylov, J. Petäjälä, and M. Sonkki, "Wireless energy transfer powered wireless sensor node for green IoT: Design, implementation and evaluation," *Sensors*, vol. 19, no. 1, p. 90, 2019.
- [127] K. M. Shams, and M. Ali, "Wireless power transfer to a buried sensor in concrete," *IEEE Sensors Journal*, vol. 7, no. 12, pp. 1573-1577, 2007.
- [128] S. Jiang, and S. V. Georgakopoulos, "Optimum wireless powering of sensors embedded in concrete," *IEEE transactions on antennas and propagation*, vol. 60, no. 2, pp. 1106-1113, 2011.
- [129] S. Jiang, S. V. Georgakopoulos, and H. Jin, "Effects of periodic reinforced-concrete structures on power transmission," in *RFID The IEEE International Conference on RFID*, pp. 16-23, 2012.
- [130] S. Jiang, S. V. Georgakopoulos, and O. Jonah, "Power transmission for sensors embedded in reinforced concrete structures," *IEEE International Symposium on Antennas and Propagation*, pp. 1-2, 2012.
- [131] N. B. Carvalho, A. Georgiadis, A. Costanzo, H. Rogier, A. Collado, J. A. García, S. Lucyszyn, P. Mezzanotte, J. Kracek, D. Masotti, and A. J. S. Boaventura, "Wireless power transfer: R&D activities within Europe," *IEEE Transactions on Microwave Theory and Techniques*, vol. 62, no. 4, pp. 1031-1045, 2014.
- [132] A. Boaventura, D. Belo, R. Fernandes, A. Collado, A. Georgiadis, and N. B. Carvalho, "Boosting the efficiency: Unconventional waveform design for efficient wireless power transfer," *IEEE Microwave Magazine*, vol. 16, no. 3, pp. 87-96, 2015.
- [133] M. A. Hossain, R. M. Noor, K. L. A. Yau, I. Ahmedy, and S. S. Anjum, "A survey on simultaneous wireless information and power transfer with cooperative relay and future challenges," *IEEE access*, vol. 7, pp. 19166-19198, 2019.
- [134] D. Allane, G. A. Vera, Y. Duroc, R. Touhami, and S. Tedjini, "Harmonic power harvesting system for passive RFID sensor tags," *IEEE Transactions on microwave theory and techniques*, vol. 64, no. 7, pp. 2347-2356, 2016.
- [135] N. Barroca, L. M. Borges, F. J. Velez, F. Monteiro, M. Gorski, and J. Castro-Gomes, "Wireless sensor networks for temperature and humidity monitoring within concrete structures," *Construction and Building Materials*, vol. 40, pp. 1156-1166, 2013.
- [136] E. Fraile-Garcia, J. Ferreira-Cabello, E. M. De Pison Ascacibar, J. F. Cenicerós, and A. V. P. Espinoza, "Implementing a technically and economically viable system for recording data inside concrete," *Construction and Building Materials*, vol. 157, pp. 860-872, 2017.
- [137] G. Loubet, E. Alata, A. Takacs, and D. Dragomirescu, "A Survey on the Security Challenges of Low-Power Wireless Communication Protocols for Communicating Concrete in Civil Engineerings," *Sensors*, vol. 23, no. 4, p. 1849, 2023.



**GAËL LOUBET (M'20)** was born in Toulouse, France, in 1994. He received the Engineer Diploma in Automatic Control and Electronics and the Ph.D. degree in Micro- and Nano-Systems, in 2017 and 2021, respectively, both from INSA Toulouse, France.

From 2021 to 2022, he was a teaching and research associate with the INSA Toulouse and LAAS-CNRS. Since 2022, he has been an Associate Professor with INSA Toulouse and LAAS-CNRS. He has authored 20 articles in refereed journals or communications in international conferences. His research interests include electromagnetic Wireless Power Transfer, wireless communication for the Internet-of-Things applications and Wireless Sensor Networks for Cyber-Physical Systems implementation and Structural Health Monitoring applications.



**ALASSANE SIDIBE (M'19)** was born in Dakar, Senegal, in 1994. He received the MSc degree in electronics of embedded system and telecommunications from the University Paul Sabatier of Toulouse in 2018.

He is currently pursuing a Ph.D. degree in communication engineering with the French company Uwinloc. He has authored and co-authored thirteen research papers in IEEE international conference proceedings and 3 articles in refereed journals. His current research interests include wireless power transmission and energy harvesting for battery-free tags, wireless sensor network and antenna design on flexible materials.



**PHILIPPE HERAIL** was born in Vernon, France, in 1998. He received the Engineer Diploma in Computer Science and Networks from the National Institute of Applied Sciences (INSA), Toulouse, France, in 2020.

He is currently pursuing a Ph.D. degree in Computer Science & Robotics. His current research interests include automated learning of planning models for autonomous agents and data efficient machine learning.



**ALEXANDRU TAKACS** (M'12) was born in Simleu Silvaniei, Romania, in 1975. He received the Engineer Diploma in electronic engineering from the Military Technical Academy, Bucharest, Romania, in 1999, and the master's and Ph.D. degrees in microwave and optical communications from the National Polytechnic Institute of Toulouse, France, in 2000 and 2004, respectively.

From 2004 to 2007, he was a Lecturer with the Military Technical Academy, and an Associate Researcher with the Microtechnology Institute, Bucharest. From 2008 to 2010, he occupied a postdoctoral position with LAAS-CNRS, Toulouse. During 2011, he was a Research and Development RF Engineer with Continental Automotive SAS France, where he was in charge of antenna design and automotive electromagnetic simulation. Since 2012, he has been an Associate Professor with the University Paul Sabatier, Toulouse, where he performs research within LAAS-CNRS. He has authored or co-authored 5 international patents, 37 papers in refereed journals, one book, one book chapter, and over 110 communications in international symposium proceedings. His research interests include the design of microwave and RF circuits, energy harvesting and wireless power transfer, battery-free wireless sensors, small antenna design, electromagnetic simulation techniques, and optimization methods.



**DANIELA DRAGOMIRESCU** (M'96-SM'15) is Professor at INSA Toulouse and LAAS-CNRS laboratory. She received the engineering degree with Magna Cum Laude from the Polytechnic University of Bucarest, Romania in 1996, the MSc in circuits design from the University Paul Sabatier, France, in 1997 and the Ph.D. degree with Magna Cum Laude in 2001 from the University of Toulouse, France.

Prof. Dragomirescu is the Deputy Director of LAAS-CNRS laboratory since January 2022. She is the IEEE Solid States Circuits French Chapter Chair. Prof. Daniela Dragomirescu was French Government Fellow of Churchill College, University of Cambridge in 2014. Daniela Dragomirescu was the Dean of Electrical and Computer Engineering Department at INSA Toulouse since June 2017 to September 2020. Prof. Dragomirescu is conducting research in the area of micro and nano systems for wireless communications with a special focus on Wireless Sensor Networks. She published more than 90 papers in journals and conferences proceedings, 2 patents and she authored 7 academic courses.